Vista Research Technical Report No. F034-TR-00-001

Final Report

SpecLab – Phase I

Prepared by:

George Papanicolaou

Dept. of Mathematics
Stanford University
Stanford, CA 94305
papanico@stanford.edu

Charles L. Rino

Vista Research, Inc.
755 North Mary Avenue
Sunnyvale, CA 94086
CRino@vrinc.com

Knut Sølna

Dept. of Mathematics
University of Utah
Salt Lake City, UT 84112
solna@math.utah.edu

Prepared for:

U.S. Air Force Office of Scientific Research
801 North Randolph Street, Room 732
Arlington, VA 22203-1977

Contract No. F49620-99-C-0049

Attention: Dr. Arje Nachman

15 May 2000

VISTA RESEARCH, INC.
755 North Mary Avenue ▪ Sunnyvale, California 94086
Telephone (408) 830-3300 ▪ Fax (408) 830-3399

AFRL-SR-BL-TR-00-

0197

REPORT DOCUMENTATION PAGE

1. AGENCY USE ONLY (Leave Blank)	2. REPORT DATE	3. REPORT TYPE AND DATES COVERED
	15 May 2000	Final 8/1/99-4/30/00

4. TITLE AND SUBTITLE

SpecLab - Phase I

5. FUNDING NUMBERS

Contract#
F49620-99-C-0049

6. AUTHOR(S)

George Papanicolaou
Charles Rino
Knut Solna

7. PERFORMING ORGANIZATION NAME(S) AND ADDRESS(ES)

Vista Research, Inc.
755 North Mary Avenue
Sunnyvale, CA 94086

8. PERFORMING ORGANIZATION REPORT NUMBER

F034-TR-00-001

9. SPONSORING/MONITORING AGENCY NAME(S) AND ADDRESS(ES)

USAF, AFMC
Air Force Office of Scientific Research
801 North Randolph St, Room 732
Arlington, VA 22203-1977

10. SPONSORING/MONITORING AGENCY REPORT NUMBER

11. SUPPLEMENTARY NOTES

Prepared in collaboration with University of Utah

12a. DISTRIBUTION/AVAILABILITY STATEMENT (see Section 5.3b of this solicitation)

Approved for public release,
distribution unlimited

12b. DISTRIBUTION CODE

13. ABSTRACT (Maximum 200 words)

This Phase I Strategic Technology Transfer Report (STTR) final report summarizes the development of a prototype interactive software environment, SpecLab, for analyzing non-stationary processes that admit local power-law representations. Standard spectral analysis procedures assume stationarity, whereas most naturally occuring processes admit random departures from strict stationarity. SpecLab estimates and synthisizes the non-stationary process by allowing both the power-law parameters and the power-law scale range to vary over a data segmentation chosen interactively by the user. The SpecLab procedures are accessible via a graphical user interface that guides the user through the steps involved in selecting data segmentations and executing the estimation procedures.

In its final form SpecLab will provides efficient user access to leading-edge analysis procedures for non-stationary processes. SpecLab is also configured to provide reproducible research that would ordinarily be available only as text, equations, and graphs.

14. SUBJECT TERMS	15. NUMBER OF PAGES
Non Stationary Processes Interactive Data Analysis	72
	16. PRICE CODE

17. SECURITY CLASSIFICTION OF REPORT	18. SECURITY CLASSIFICATION OF THIS PAGE	19. SECURITY CLASSIFICATION OF ABSTRACT	20. LIMITATION OF ABSTRACT
U			

Final Report:
SpecLab Phase I

George Papanicolaou[1] Chuck Rino[2] Knut Sølna[3]

May 15, 2000

[1]Department of Mathematics, Stanford University, Stanford CA 94305, *papanico@math.stanford.edu.*

[2]Vista Research, Inc., 755 North Mary Avenue Sunnyvale, CA 94086, *CRino@vrinc.com.*

[3]Department of Mathematics, University of Utah, Salt Lake City UT 84112, *solna@math.utah.edu.*

Abstract

This Phase I Strategic Technology Transfer Report (STTR) final report summarizes the development of a prototype interactive software environment, SpecLab, for analyzing non-stationary processes that admit local power-law representations. Standard spectral analysis procedures assume stationarity, whereas most naturally occuring processes admit random departures from strict stationarity. SpecLab estimates and synthesizes the non-stationary process by allowing both the power-law parameters and the power-law scale range to vary over a data segmentation chosen interactively by the user. The SpecLab procedures are accessible via a graphical user interface that guides the user through the steps involved in selecting data segmentations and executing the estimation procedures.

In its final form SpecLab will provides efficient user access to leading-edge analysis procedures for non-stationary processes. SpecLab is also configured to provide reproducible research that would ordinarily be available only as text, equations, and graphs. The Phase 1 prototype demonsrates all the essential features of a marketable software product to be developed under a Phase II effort.

The report is organized as follows. Chapter 1 provides introductory background information and summarizes the developmental Phase I accomplishments against the content of the original plan. Chapter 2 provides a detailed functional description of the prototype software that comprises SpecLab Version 1. Chapter 3 summarizes the proposed Phase II STTR effort that will develop the final SpecLab product. Chapter 4 reproduces the paper "Wavelet Based Estimation of Local Kolmogorov Turbulence," by G. Papanicolaou and K. Sølna, which has bee submitted for publication. The paper summarizes the theoretical underpinnings of SpecLab and demonstrates the reproducible research capability. Chapter 5 reviews the relation of standard spectral analysis procedures and wavelet-based estimation.

Contents

Chapter 1

SpecLab Overview

1.1 Introduction

Stochastic models that incorporate non-stationary structure through long-range correlations have been the focus of much attention. Such models have been used to analyze communications data involving local area networks, video, wide area networks, and common channel signaling. In geophysics long-range dependencies have been found in the fluctuations of parameters that characterize the earth's crust. Finally, stochastic models that incorporate long-range dependence are fundamental in the analysis of turbulent flow data. This latter application provided the focus of and motivation for developing SpecLab.

The theory of stationary stochastic processes is well developed, but deviations from stationarity are crucial in the aforementioned applications and in many other, if not most, applications that involve stochastic processes. Yet, modeling and estimation of non-stationary processes is neither well developed nor an integral part of mainstream data analysis procedures. SpecLab makes extensive use of the wavelet transform, to provide spatially localized information about the essential frequency content of the data. An important objective of the SpecLab development is to make this recent progress in the development of practical methods for dealing with non-stationary long-range dependent processes available and accessible to a broad spectrum of potential users.

To achieve this objective, we have structured SpecLab as an interactive software environment for data analysis, estimation and synthesis of local power-law processes, which are described in more detail below and in Chapter 4. Local power-laws provide a robust, well understood model for the development. The interactive structure of SpecLab allows data exploration by identifying a representative power-law structure and synthesizing realizations of the data from the estimated model parameters. SpecLab also serves as a learning environment for fractals, multifractals and local power laws in general. Finally, it serves as a tool for reproducible research in the subject area. Reproducible research is intended to make the data and the analysis procedures that underlie research reports available along with the textual and graphic descriptors.

1.2 Local power-law processes

Fractional Brownian motion (fBm) represents a local power-law process in its simplest form. Fractional Brownian motion, B_H, is a non-stationary Gaussian process with stationary increments. The variance of the stationary increment process is characterized by the structure

function

$$E[(B_H(x) - B_H(x - \Delta x))^2] \quad = \quad \sigma^2 |\Delta x|^{2H}. \tag{1.1}$$

The Hurst exponent H determines the correlation distance for the increments of the process while σ^2 establishes the absolute level of the correlation. Ordinary Brownian motion corresponds to $H = 1/2$ and its consecutive increments can be shown to be independent. Increasing and decreasing values of the Hurst exponent correspond to positive and negative correlations, respectively (see Section 4.2). Fractional Brownian motion is self-similar since $B_H(x)$ and $a^H B_H(x/a)$ have the same distributions. The process is essentially invariant with respect to scaling and, thus, contains structural features on all scales. This attribute reflects the long-range dependence aspect of the process. Although the structure function (1.1) has a power-law form, the complementary spectral-domain power law $C\omega^{-(2H+1)}$ is the source of the definition. The spectral strength C is related to the Hurst exponent and σ (see Chapter 5).

The local power-law model used in SpecLab generalizes the fBm model in two ways. First, the power law parameters σ and H are not constant, but vary slowly with respect to location x. These variations are modeled as secondary stochastic processes. Second, the model (1.1) is applied only over a subset of scales: $x_{in} < x < x_{out}$, which is called the inertial range in turbulence theory. Turbulence theory is an important application of the fBm model. Kolmogorov's scaling law yields a spectral index for temperature fluctuations that corresponds to $H = 1/3$ in the inertial range. However, real data typically show a multifractal behavior as manifest by variations in σ and H as well as variations in the inertial range itself. SpecLab is designed to estimate these variations.

Selection of an appropriate bias-variance trade-off is critical to the estimation procedure. For example, if the mean power-law parameters are estimated over segments of fixed length, the fluctuations in the estimate decrease with the length of the segments; however, the bias increases with the length of the segments since intrinsic variations in the power-law parameters are smoothed out. The local power-law model and the scheme designed to handle the above estimation problem are described in more detail in Chapter 4.

1.3 Summary of Phase I STTR Effort

In our Phase I STTR proposal the following classes of analysis routines were identified as the functional units of a viable software environment for analyzing non-stationary power-law processes.

Data analysis and simulation

These are basic routines that transform the data, perform wavelet scale-filtering, and display the data in various ways. This set of procedures also contains routines that simulate local power-law processes. The most elaborate of these routines is the fBm simulator.

Scale spectra estimation

These are routines that analyze the transformed data obtained from the basic analysis and simulation procedures. The collection includes routines that estimate scale spectra, the inertial range, and the power-law parameters. Scale spectra are described in 4.2.2. Note that the power-law parameter estimates conain an estimation error that depends on the segmentation of the data vector. This error is approximately removed by the filter described in Section 4.4.

Segmentation analysis

The first group of routines in this set is designed to extract an optimal smoothing of the power law parameters derived from the scale spectra associated with a given segmentation. The smoothing is based on an estimate of the spatial correlation of these parameters over segments, as described in Section 4.4.3. SpecLab includes tools that support the estimation of the structure function that defines the spatial correlation for a given power-law process realization.

The second group of routines in this set provides guidelines for choosing an optimal prior segmentation of the signal. The optimal segmentation balances bias and variance as discussed in the introductory description.

Fourier spectral estimation

For completeness and as a means of relating the SpecLab analysis to results obtained from conventional analyses, standard spectral analysis routines are included. The relations are summarized in Chapter 5.

Interactive interface and intermediate level routines

This is a graphical user interface (GUI) that allows the user to apply SpecLab routines in a user-friendly way. Intermediate-level routines that carry out complete subtasks like optimal smoothing of spectral parameters are invoked by the GUI. The intermediate level routines make it convenient for the user to identify the key computational procedures in SpecLab and how they can be tailored toward specialized applications.

Demos

These are Matlab demonstration scripts that perform end-to-end analyses of specific data sets. They serve as an introduction to SpecLab and provide the SpecLab user with practice exercises to explore its capabilities.

Our Phase I plan has been successfully completed. The SpecLab prototype software provides an interactive Matlab-based software environment for analysis of local power-law processes. Users can select sample data sets, generate synthetic data sets, or import data of their own choosing. SpecLab procedures will display the input data, its spectrum, and various parameters that will assist in the subsequent processing. The package is designed to provide the user with a systematic method for identifying appropriate inertial ranges and the intrinsic variation in the power-law parameters. The SpecLab prototype developed under the Phase I STTR uses Matlab's GUI facilities and Matlab's system for on-line documentation and help. It requires both Matlab and the Wavelet Tool Box, but, under the proposed Phase II effort, stand-alone Unix and PC versions will be developed.

The SpecLab estimation procedures have been demonstrated to work well both with real and synthetic data. Moreover, all of the results discussed in Section 4 can be reproduced with SpecLab, which demonstrates its reproducible research capability. SpecLab has been implemented with a GUI. This task was deemed sufficiently important that we accelerated the development beyond the original Phase I plan.

Functions that have not yet been implemented include (i) *Adaptation,* which is a procedure to help the user select a prior segmentation, (ii) *Measurement noise,* which is a procedure that quantifies measurement noise in the data, and (iii) *Spectral comparison.* The material described in Chapter 5 covers (iii). The incorporation of these remaining functions is discussed in Chapter 3.

Chapter 2

SpecLab Version I

2.1 Introduction

SpecLab is a Matlab-based prototype software environment designed to illustrate the essential elements of an interactive analysis tool for non-stationary processes. It is based on the work done by G. Papanicolaou and K. Sølna with the collaboration of V. Kruger and C. Rino of Vista Research and D. Washburn of the Air Force Lab at Kirtland Air Force Base. SpecLab was developed and written by K. Sølna. The software as described below is available via anonymous ftp upon written request to the authors. The remainder of this section takes the form of a preliminary user's guide for SpecLab Phase I.

2.2 Running SpecLab

SpecLab is written in interactive Matlab version 5.3. This user's guide assumes that the user is running Matlab and is familiar with its operation and data structures. It is also necessary to have the Matlab Wavelet Toolbox installed. SpecLab will run under the Unix/Linux or the PC/NT versions of Matlab. The startup script will define the appropriate environment. In the remainder of this section we assume that the SpecLab directory has been downloaded and uncompressed.

With Matlab running, change directories to 'SpecLab/Lab' to set up the program environment. The procedure is the same for Linux or PC versions. To start SpecLab type 'SpecLab'.

2.2.1 Reading or simulating a data vector

After typing SpecLab in Matlab the user will be presented with the following menu:

CHOOSE INPUT:
HELP
BINARY file with data-vector
ASCII file with data vector
SIMULATE a process
DEMO
QUIT

The first option initiates an on-line help utility. The second and third options load existing binary or ASCII files. The fourth option allows the user to synthesize a data vector with prescribed local power-law characteristics. The demo option will walk the user through the various processing steps to illustrate the functional elements of SpecLab.

For the second or third options a menu appears that identifies the following precomputed data vectors:

- pure Brownian motion
- Brownian motion with tapered spectrum
- a pure Kolmogorov process with $H = 1/3$
- local Brownian motion
- typical aerothermal data (the data set described in Chapter 4)

The user can alternatively specify the name of a file that contains data stored as a sequence of numbers in a one-column format. The routines implementing file communication are located in subdirectory 'SpecLab/fileio.'

The simulation option initiates a sequence of menus that input the following local power-law parameters:

- length of data vector
- inner scale
- outer scale
- correlation length of parameter variations
- mean Hurst exponent
- fluctuations of Hurst exponent H
- fluctuations of the log intercept $\log(\sigma^2)$

The parameters H and σ^2 can be chosen to be deterministic or random.

Finally, choosing the demo option initiates a workout that illustrates the estimation of a local power-law process, as described in Section 2.5.

2.2.2 Analyzing and plotting data

Once SpecLab has loaded or synthesized a data vector, the user is presented with a menu that identifies the various procedures that can be performed on the data vector as summarized below:

CHOOSE INPUT:
HELP
CHOOSE segmentation
ESTIMATE inertial range
ESTIMATE model for power law parameters
PLOT process
PLOT wavelets
PLOT scale spectrum (color)
PLOT scale spectrum (graphs)
PLOT power law parameters
PLOT smoothed power law parameters
PRINT current plot
SAVE current data
FILTER data
RETURN to input menu
QUIT

As a guide to the choices, recall that estimating the local power-law model parameters involves three steps:

(i) Segmentation of the raw data vector into a specified number of *equal-length* segments.

(ii) Estimation of inertial range for each segment and of the power-law parameters for each segment.

(iii) Estimation of the structure-function model that characterizes the correlation of the of the power-law parameters for the segmentation.

Selecting the second, third, and fourth entries in sequence carries out these operations. The main menu also has a number of options for plotting the data that can be executed before and during the power-law parameter estimation. The action choices are described in more detail below.

(i) Segment the data

Selecting the segmentation option initiates a secondary menu with the following choices:

(a) Enter the number of *equal-length* segments.

(b) Display the space-scale spectra in a color format.

(c) Display the scale spectra as graphs.

(d) Return to main menu with current segmentation.

The scale spectra are calculated over each segment and stored in the SpecLab data structure; see Section 2.3. Once this step has been performed, the scale-spectra displays can be initiated from the main menu. The *default* segmentation is one segment.

(ii) Estimate inertial range

Selecting this estimation option initiates a secondary menu with the following choices:

(a) Estimate the inertial range.

(b) Specify the inertial range.

(c) Display the space-scale spectra in a color format.

(d) Display the scale spectra as graphs.

(e) Return to main menu with current segmentation.

For option (a) the interial range estimates are computed automatically based on comparison of the scale spectra with pure fractional Brownian motion; see Section 4.4.2. For option (*b*) the user chooses a constant segmentation that is applied to all data segments. The *default* inertial range uses all available scales.

(iii) Estimate structure function

The stochastic variation of the power-law parameters from segment to segment is modeled by independently fitting an exponential structure functions of the form

$$w + v(1 - \exp(-\Delta x/l))$$

to H and $\log(\sigma^2)$. Here l is the 'correlation range,' w is the 'intercept,' v is the 'variance' and Δx converts the lag number to sample units. The user is supported in

choosing the appropriate structure function with displays that compare the empirical structure function calculated from the data with the default model (exponential) structure function. The user can modify the parameters in the model interactively in order to improve the fit via a secondary menu with the following options:

- Change correlation range.
- Change variance.
- Change intercept.
- Change max variogram lag.
- Accept current parameters.

Note that if the number of segments, and hence the length of the power-law parameter processes, is too short, then the default structure function model is used. The default model corresponds to constant power-law parameters, which is also assumed if the estimation of structure function step is omitted.

(iv) Scale filter data

Scale filtering is a process by which the data are reconstructed using only a selected range of the scale spectra values. The operation is useful as a preprocessing operation to remove spurious contamination of real data vectors.

Choosing this option brings up a secondary menu with the following options:

- Select scale range.
- Display scale-filtered process.
- Return with filtered data replacing original data.

2.3 SpecLab data structure

The data vector processed by SpecLab is a data structure that accumulates inputs as the various operations are performed. The scripts in SpecLab communicate using this data structure. An example of a data structure is given below

```
Z =

          data: [65536x1 double]
         wavec: [65536x1 double]
         wavel: [12x1 double]
          nseg: 32
       scspect: [32x10 double]
      inertial: [32x2 double]
       parproc: [32x2 double]
       filtpar: [0.0026 0 7. 0.0463 0 8.]
   filtparproc: [32x2 double]
   trueparproc: []
```

The field values (see also Section 5.2.2) contain the following objects:

data	the data vector
wavec	the vector c in Matlab's wavelet decomposition
wavel	the vector l in Matlab's wavelet decomposition
nseg	number of segments in the uniform segmentation of the data vector
scspect	the scale spectra for the given data vector and segmentation
inertial	the estimated inertial ranges for the given segmentation
parproc	the power-law parameter estimate based on the scale spectra and estimated inertial ranges
filtpar	the parameters in the structure-function models for the power law parameters
filtparproc	the filtered power-law parameters
trueparproc	if the data vector was simulated the true parameter processes are stored here

2.4 SpecLab directory structure

The SpecLab directories and files are

Lab InitZ Main SpecLab
demoAero demoBm demoInert demoKol demoLfBm
specpath startup

display displayP displayS displaySyn displayVario displayW displayX

fileio ReadSpec WriteSpec getdat writedat

SpecLab

options HelpInput HelpSpec InertialSpec ProcSpec ScaleSpec
ScfiltSpec SmoothSpec SynthSpec VarioSpec

demo aero pause showinput showmenu

tools

inertialest
GetInertial Inertial MakeRefres Refres

varioest
GetVario VarioEst regmodel

spectest
GetParproc Linreg Spect hfunc

filter
Filt_Par Scale_Filt Taper

simulation
SegSim SimExp sim_ob simcoef vfunc

The scripts are documented in Appendix A.

2.5 The "Workout"

The workout shows how SpecLab commands can be used to generate all the figures in Section 4. The script that implements the workout is 'aero.m' and is located in directory 'SpecLab/aero.' The demo illustrates the steps involved in estimating a local power-law model. By looking at the script itself the user can get information about how the intermediate level SpecLab routines implement the estimation steps. The user starts the workout by choosing the option 'demo' in the input menu described in Section 2.2.1. Starting the demo gives the following figures

Figure 4.1 Displays the data vector. The data vector is 'demoAreo' located in directory 'SpecLab/Lab.' This data vector can be analyzed independently by choosing fhte second or third options in the input menu described in Section 2.2.1.

Figure 4.2. Next, the user is presented with the main menu given in Section 2.2.2. Choosing the menu option 'PLOT wavelets' creates the figure.

Figure 4.3. The user is asked to choose the main menu option 'CHOOSE segmentation' and then give the number of segments. Choosing the 'plot scale spectra (graphs)' option creates the figure.

Figure 4.7. The user is asked to choose the main menu option 'ESTIMATE inertial range' and then choose the 'estimate inertial range' option. Choosing the 'plot inertial scale spectra (graphs)' option creates the figure.

Figure 4.8. By choosing the main menu option 'PLOT Power law parameters' the user obtains the figure with the estimated parameter processes. Note that the parameter processes have been truncated so that only the parameters in the latter, high-turbulence regime are given.

Figure 4.10. Finally, by choosing the main menu option 'PLOT Smoothed power law parameters' the user obtains the figure with smoothed parameter processes. Before doing the smoothing of the parameter processes the structure function for the parameter processes need to be estimated. In the workout these were chosen to be the ones used in [24], when analyzing another data set these must be estimated choosing the 'ESTIMATE model for power-law parameters' option in the main menu.

Chapter 3

Phase II Plan

3.1 Introduction

The prototype SpecLab environment demonstrates all the essential elements of an interactive analysis tool for non-stationary local power-law processes. In its present form, however, it has a number of limitations that would preclude its use by all but knowledgeable users. Under a Phase II effort SpecLab would be converted into a more general and complete software environment, together with Web-based documentation and interactive capability. The general structure of SpecLab lends itself readily to these enhancements.

3.1.1 Analysis and synthesis of local power laws

We have emphasized that while the theory of stationary stochastic processes is well developed, there are few widely available utilities for analyzing non-stationary process. Non-stationary processes by their very nature require adaptive processing. Thus, we believe that one of the most important features of SpecLab is its capability for interactive and adaptive processing. This, in turn, places more critical demands on user support. SpecLab ultimately will make these techniques available in a robust and user-friendly software environment. Interactive analysis and synthesis for identification and replication of non-stationary effects in a large class of fractal and multifractal processes are novel features that SpecLab will provide. SpecLab also contains a number of features that extend beyond those associated with local power laws. With the proposed software environment these features can be used for more general problems. Thus, the focus on local power-laws is not overly restrictive.

3.1.2 Reproducible Research

Reproducible research was pioneered in the development of the software package Wavelab [4]. The stated objective was to make the full content of research available via a complete software environment that implements the computational procedures used to generate reported numerical results. The development of SpecLab will fully preserve this capability. While the SpecLab reproducible research umbrella is specific to the analysis of non-stationary processes using a local fBm-based power-law model, the structure is a template for distinctly different applications that are based on interpretive analysis tools.

3.1.3 SpecLab as a learning tool

Fractal and multifractal processes have been the subject of much recent interest. SpecLab will serve as a learning tool for users who want to understand such processes. Through that understanding we expect new applications to emerge. A key aspect of SpecLab is analysis and processing using the wavelet transform. The package contains user friendly procedures for filtering in scale and time and visualization of the considered process based on this transform. Thus, SpecLab can also serve as an introduction to wavelet applications.

3.1.4 Creating a portable software environment

The creation of the world-wide Web has revolutionized information exchange. We will make use of the Web to provide easy access to SpecLab and its documentation. By making the product easily available in a platform-independent form, the impact of research and developed software is enhanced enormously. We expect that the development of this aspect of the software package will formalize an emerging trend at universities and research institutes.

3.2 Project outline

Under the Phase II effort the utilities described below would be developed.

3.2.1 Extended user guide

- **SpecLab Web page.** A Web page will be developed that will give background information about SpecLab and its functionality. It will be based on an updated version of the information in this Phase I report for SpecLab. That is, the Web page will identify the SpecLab objectives, give information about locally stationary processes, and document the software along the lines of an enhanced HTML version of Chapter 2. The visitor to the Web page will also be able to download relevant papers, such as [19, 24, 25].

  The Web page will give instructions on how to download the software. Both compiled stand-alone versions and MatLab scrips (as SpecLab is now configured) will be made available. Both versions can be used in Windows or Linux-based environments. User groups can be created for the exchange of ideas and techniques involving SpecLab and similar software tools, data sets etc.

- **SpecLab manual.** From the Web page the user will be able to download a manual that contains the information on the Web page itself, that is, a description of all subroutines in SpecLab, information about downloading SpecLab, starting SpecLab etc. The manual will also contain detailed documentation of the examples on the Web page, as well as detailed information about the functions in SpecLab and the software architecture.

- **Workouts.** The downloaded software will contain a set of interactive examples that will provide "guided tours" through specific applications of SpecLab. The Phase I version of SpecLab does this for an aerothermal data set. These workouts will provide a complete analysis of important data sets and serve as an exended introduction to SpecLab. We envision at least four workouts: one based on the aerothermal data set, one based on Internet traffic data, and two based on numerically generated data sets.

- **Online help.** At every stage in the execution of SpecLab the user will have access to online help in the form of hyperlinks to the relevant parts of the formal documentation.

3.2.2 Portability

Users will be able to download the package will be available via anonymous ftp or directly from the Web page. There will be both Linux and Windows versions of SpecLab. The user can choose to download either a compiled version or a version based on Matlab scripts. The compiled version will not require the user to have Matlab. The Matlab version, on the other hand, will enable the user to tailor the Matlab scripts to specialized processing tasks. This activity will include replacing Matlab's toolbox procedures for computing the wavelet transform with the corresponding routines in the freely available software package Wavelab [13].

3.2.3 GUI, visualization and data manipulation

- The graphical user interface (GUI) will be improved so that it better guides the user through different processing options.
- Interactive parameter input will be improved. For instance, the user will be able to select the magnitude of the parameters on a continuous scale by using dials and bars rather than from the set of discrete values in the current version.
- The user will be able to employ the mouse to select a subset of the signal from a time frequency plot and continue processing with this subset.
- The routines for data input and validation will be improved as a way to facilitate input of data in various formats.

3.2.4 Adaptation

Estimation of the locally stationary spectral parameters is based on a prior segmentation of the data. This is a key step. A tool that supports the choice of the prior segmentation will be of great interest, not only in SpecLab, but also in many other signal processing applications. In version 1 of SpecLab the segmentation is done manually. In the final version procedures will be implemented to specify a *range* of segmentations. A new component of SpecLab will then look for an optimal segmentation within this range. This new component of SpecLab will in part be based on the framework set forth by Mallat et al. in [17]. The segmentation problem is a fundamental issue in signal processing. However, how to do it well is still largely an open question. The promising approach introduced by Mallat et al. in [17] is based on an optimal compression of the covariance operator in a suitable basis. SpecLab provides a framework for solving this important problem.

3.2.5 Simulation

Some users may be interested mainly in using SpecLab for simulation of local fractional Brownian motion. Thus, simulation of stochastic processes is another module within SpecLab that will be important. The current simulation algorithm is based on a fast dyadic refinement algorithm [23]. The proposed activity involves the following tasks:

- The simulation algorithm will be optimized for speed. This involves fine tuning of the default parameters chosen in the simulation algorithm, and also further algorithmic development. The refinement scheme in the current simulation algorithm will be embedded in a divide-and-conquer framework that will further increase the efficiency of the algorithm. Efficiency will be improved both with respect to computational cost and in terms of use of the memory hierarchy.

- Rather than having to use default parameters, the user will be given the option of specifying a desired precision. With lower precision, i.e., larger deviations from the specified power law, the simulation will be faster.

- A separate menu-driven tool that facilitates the simulation will be developed. The user will be able to simulate multiple realizations in parallel and carry out simulations in a batch mode. This module will make use of the improved facilities for parameter input.

- The user will be given some flexibility in terms of choosing the stochastic model. It will be possible to simulate point samples of fractional Brownian motion or fractional Brownian motion that has been filtered so that the simulated values correspond to local integrals of pure fractional Brownian motion. In addition the user will be able to simulate local fractional Brownian motion where power law parameters are non-constant.

- The procedure for simulation of local fractional Brownian motion will be improved. In Version I of SpecLab this was done with a strong Markov approximation. This will be relaxed in version II by means of the divide-and-conquer step in the new algorithm.

3.2.6 Variogram estimation

An important task in applied signal processing is the choice of an appropriate model for the variogram or structure function. In SpecLab the variogram must be estimated for the parameter processes that come from the initial segmentation. This subtask in SpecLab will be developed further. The user will be able to modify parameters in a continuous fashion, exclude data points, modify the set of points used in the estimation, etc. The objective is to provide a state-of-the-art algorithm for this purpose that has at least the functionality of existing geostatistical packages. Since this is an important task, the user will be given the opportunity to carry out variogram estimation for an arbitrarily specified data set, not only the parameter processes.

3.2.7 Bias, precision and wavelets

The current version of SpecLab is based on Haar wavelets. In the final version the user will be given the option of using other types of wavelets. Using other wavelets is of particular importance for extended signals where the non-stationary aspect is relatively low and the desired precision for the parameter estimates is very high.

For small sample sizes (say with only a few spectral samples) or non Haar wavelet based estimation the bias in the parameter estimation must be computed numerically. This will be done a priori and the bias looked up in a table-lookup procedure. In Version 1 of SpecLab an analytic expression for the bias was used; this assumes, however, that the estimation is based on Haar wavelets.

In the new version of SpecLab the user will also be given the option to plot confidence bands for the estimated power law parameters. The calculation of the variability of the estimates will be based on a similar table-lookup procedure as the one pertaining to the bias correction.

3.2.8 Extension to exponential model

So far SpecLab has been tailored to local fractional Brownian motion. In the new version the user will be given the option of choosing as a model an exponentially correlated Gaussian process as well. This will significantly increase the set of applications in which SpecLab can be used as a tool. The three parameters in the exponential model (variance, correlation range, and white noise component) will be modeled as being locally stationary and estimated similarly to the way the local power law parameters are estimated. This work includes further theoretical development as well as new implementation and testing on some real data sets. These data sets can, for instance be taken from the atmospheric data collection effort [34].

3.2.9 Incorporating prior information

The most important turbulence parameter, the Hurst exponent, takes on values in the range in between zero and one. This constraint will be included via a non-informative prior distribution in a Bayesian estimation scheme. It will also be considered to include more general prior distributions on *both* turbulence parameters, the Hurst exponent and the intensity, for better handling of small data sets and also for fast adaptation.

Chapter 4

Theory

4.1 Introduction

Stochastic processes that are approximately stationary and have approximately power law spectral densities arise frequently in modeling atmospheric turbulence, financial data, geophysical data, etc. How can we estimate the variable power law behavior of the spectral densities from data? The analysis will depend on how we segment the data and on how we choose the range of scales, or frequencies, over which we look for a power law fit. In this paper we address these issues using fractional Brownian motion as the underlying stochastic model whose parameters are estimated locally by wavelet scale spectra. We then apply the theory to atmospheric turbulence data. This data was first analyzed in Washburn et al. [34] and subsequently in Papanicolaou, Sølna, and Washburn [25]; Rossi, Kaiser, and Washburn [30]; Papanicolaou, Sølna, Rino, and Kruger [19]. We provide here a general framework for estimating local power law processes with wavelets and a large part of the mathematical background needed for its justification.

In Section 2 we introduce Fractional Brownian motion as a model for turbulence and discuss the wavelet based scale spectrum that can be used for spectral estimation of such processes.

In order to deal with approximate stationarity and approximate power law spectra we need a good understanding of the estimation issues for stationary, power law processes, like fractional Brownian motion. Previous work on the statistics of wavelet scale spectra of fractional Brownian motion can be found in Flandrin [7]; Tewik and Kim [33]; Abry, Goncalves and Flandrin [1]; Wornell [36]; Peltier and Levy-Vehel [27]; Wang, Cavanaugh and Song [35]. After analyzing the data, we provide in Section 6 a brief but complete analysis of these statistics that is based on a general formula for the covariance of the Haar wavelet coefficients (equation (4.13)). A central limit theorem for the estimators of the power law parameters also follows readily from the covariance formula. When Fourier spectra are used the statistical analysis of global power law processes is given in Robinson [32] and an analysis of estimators for the exponent of the power law is given in Hall, Koul, and Turlach [11]; Kent and Wood [16]. We use wavelet scale spectra because they provide a time-scale decomposition of the data that is well suited to power law processes, whether they are stationary (have stationary increments) or not. A comparison of power law estimation based on wavelet scale spectra and on Fourier spectra, in the stationary case, is given in Abry el al. [1].

In Section 3 we introduce the atmospheric data, and carry out a preliminary scale spectral analysis using the Haar-wavelet basis. This analysis suggests that nonstationary effects are indeed important for this data set. The range of scales over which the spectrum can be

modeled as a power law, the inertial range, as it is called in turbulence theory, varies with spatial location and, in addition, the estimated power law parameters depend on location.

In Section 4.4.2 we address the issue of choosing the range over which to fit the power law by regression. We do this by using the fractional Brownian motion as a model locally. Since the process is only locally stationary, power law parameters must be estimated based on relatively short spatial segments. In Section 4.4.3 we show how to remove the variability of the estimated power law parameters that is due to the finiteness of the segments. The filtering that we do here is used frequently in geostatistics (Ripley [32]; Cressie [3]).

In Section 5 we return to the atmospheric data set and use the framework introduced in Section 4 for estimation of its scale spectrum. We segment the data into intervals over which they are approximately stationary without resorting to a full segmentation search as in the method of Mallat, Papanicolaou and Zhang [17] that is based on the local cosine transform. To avoid the global search we must have a rough estimate of the size of the intervals of stationarity, which for the aerothermal data set we get from a variogram analysis of the wavelet coefficients [20]. Another case where the intervals of stationarity are known approximately is analyzed in Asch el al. [2] using the local Fourier transform.

Finally we show some simulations from the estimated model that assess the overall relevance of our analysis. The main point of our analysis is that we are able to identify the local variations of the power law parameters, the Kolmogorov turbulence law, which arise from large scale atmospheric phenomena. The analysis should be applicable to other data sets, financial data for example, where departure from stationarity needs to be quantified.

4.2 Scale spectrum of Fractional Brownian motion

4.2.1 Fractional Brownian motion

We shall model 'pure' power law processes by fractional Brownian motion (fBm), $\{B_H(x); x \geq 0\}$, introduced by Mandelbrot and Van-Ness [20]. It is a Gaussian process with mean zero, stationary increments and covariance

$$E[B_H(x)B_H(y)] = \frac{\sigma^2}{2}(|x|^{2H} + |y|^{2H} - |x-y|^{2H}) \tag{4.1}$$

with $0 \leq H \leq 1$ and σ parameters. Its structure function is

$$E[(B_H(x) - B_H(x-\Delta x))^2] = \sigma^2|\Delta x|^{2H},$$

and it is conditioned to be zero at the origin: $B_H(0) = 0$. The so called Hurst exponent H determines the correlation of the increments. The covariance of future increments with past ones is

$$\begin{aligned}\rho_H(\Delta x) &= E[(B_H(x) - B_H(x-\Delta x)) \\ &\quad \times (B_H(x+\Delta x) - B_H(x))] = \sigma^2(2^{2H-1} - 1)|\Delta x|^{2H},\end{aligned}$$

which is independent of x. When $H > 1/2$ this quantity is positive so if the past increment is positive, then on average the future increment will be positive. Feder [5] calls this persistence. When $H < 1/2$ we have an antipersistent process with a positive increment in the past making a positive increment in the future less likely. Ordinary Brownian motion corresponds to $H = 1/2$. In this case future and past increments are independent. Of special interest here is $H = 1/3$ which corresponds to the Kolmogorov scaling law (Monin and Yaglom [21]).

Fractional Brownian motion has stationary increments but is not itself stationary. However, as shown in Abry et al. [1] for example, it is possible to assign a pseudo-spectrum to it by cutting off the low frequencies. Let

$$X = B_H * \psi$$

with star denoting convolution and ψ a function that integrates to zero so that its Fourier transform Ψ vanishes at zero frequency. The process X is stationary and its power spectrum is

$$P_X \quad \propto \quad \sigma^2 |f|^{-(2H+1)} |\Psi(f)|^2 .$$

Since we usually observe power law processes through a filter that cuts off very low frequencies, we can associate with B_H the power law spectrum

$$\widetilde{P}_{B_H} \quad \propto \quad \sigma^2 |f|^{-(2H+1)} .$$

In the Kolmogorov case $H = 1/3$ the spectrum is $\sigma^2 |f|^{-5/3}$ over some range of frequencies, called the inertial range.

Fractional Brownian motion is self-similar since $B_H(x)$ and $a^H B_H(x/a)$ have the same finite dimensional distributions for all a. We next discuss estimation of fBm, or a pure power law process. In Section 4.4 we generalize the estimation procedure to locally stationary power law processes.

4.2.2 Haar wavelets and scale spectrum

We want to carry out a spectral analysis of the process, given as a finite set of data, and to fit the estimated spectrum to a power law. For this purpose **scale** spectra, rather than Fourier spectra, will be used. Scale spectra are a natural and flexible tool for self-similar processes (Kaiser [15]; Abry et al. [1]). The scale spectrum is defined in terms of the coefficients of the data in a wavelet basis. We will use the Haar wavelet basis although other bases could have been used as well (Goncalves and Abry [9]). Haar wavelet based estimators are sometimes related to classical ones, as is in particular the Allan variance estimator for the slope of the log of the spectral density (Percival and Guttorp [28]).

Let Y denote the process for which we want to compute the Haar wavelet coefficients. Denote the *approximation* coefficients at level zero by $X = (a_0(1), a_0(2), ..., a_0(2^M))$. These are defined by

$$a_0(n) \quad = \quad \int_{n-1}^{n} Y(x)dx \ .$$

Given this level zero representation, the data, we construct successively its wavelet coefficients with respect to the Haar basis as follows. Let

$$\begin{aligned} a_1(n) \quad &= \quad \frac{1}{\sqrt{2}}(a_0(2n) + a_0(2n-1)) \qquad (4.2) \\ d_1(n) \quad &= \quad \frac{1}{\sqrt{2}}(a_0(2n) - a_0(2n-1)) \ , \quad \text{for} \quad n = 1, 2..., 2^{M-1} \end{aligned}$$

be the smoothed signal and its fluctuation, or detail, at the finest scale. Note that the *detail* vector d_1 contains every other successive difference of the data. This process of averaging and differencing can be continued by defining

$$\begin{aligned} a_2(n) \quad &= \quad \frac{1}{\sqrt{2}}(a_1(2n) + a_1(2n-1)) \\ d_2(n) \quad &= \quad \frac{1}{\sqrt{2}}(a_1(2n) - a_1(2n-1)) \ , \quad \text{for} \quad n = 1, 2..., 2^{M-2} \end{aligned}$$

and in general

$$\begin{aligned} a_j(n) &= \frac{1}{\sqrt{2}}(a_{j-1}(2n) + a_{j-1}(2n-1)) \\ d_j(n) &= \frac{1}{\sqrt{2}}(a_{j-1}(2n) - a_{j-1}(2n-1)) \ , \quad \text{for} \quad n = 1, 2..., 2^{M-j} \end{aligned}$$

for $j = 1, ..., M$. The data vector X can then be reconstructed from $a_M, d_M, d_{M-1}, ..., d_1$ since from equations (4.2) we have

$$\begin{aligned} a_0(2n) &= \frac{1}{\sqrt{2}}(a_1(n) + d_1(n)) \\ a_0(2n-1) &= \frac{1}{\sqrt{2}}(a_1(n) - d_1(n)) \ , \quad \text{for} \quad n = 1, 2..., 2^{M-1} \end{aligned}$$

and now a_1 can be replaced by sums and differences of a_2 and d_2, etc.

The detail coefficients at level j can alternatively be expressed as

$$d_j(n) = \frac{1}{\sqrt{2^j}} \int_{-\infty}^{\infty} \psi(x/2^j - n) Y(x) dx$$

with the mother wavelet defined by

$$\psi(x) = \begin{cases} -1 & \text{if} \quad -1 \leq x < -1/2 \\ 1 & \text{if} \quad -1/2 \leq x < 0 \\ 0 & \text{otherwise} \end{cases} .$$

The difference coefficients correspond to probing the process at different scales and locations, with n representing location and j scale. From the self-similarity of fractional Brownian motion it follows that for such a process $E[d_j(n)^2] \propto 2^{j(2H+1)}$.

The scale spectrum of X relative to the Haar wavelet basis is the sequence S_j defined by

$$S_j = \frac{1}{2^{M-j}} \sum_{n=1}^{2^{M-j}} (d_j(n))^2 \ , \quad j = 1, 2, ..., M. \tag{4.3}$$

For fractional Brownian motion the log of the scale spectrum is approximately linear in the scale j. As discussed further in Section 6 this can be used to estimate the parameters of the process by regression It is easily verified from the definitions above that the l^2 norm of the data vector X can be written as

$$\sum_{n=1}^{2^M} (a_0(n))^2 = (a_M)^2 + \sum_{j=1}^{M} 2^{M-j} S_j \ ,$$

which is a way of expressing the orthogonality of the decomposition of X into a_M and the d_j, $j = 1, ..., M$.

The scale spectral point S_j is the mean square of the detail coefficients at scale j. The spectrum can therefore be interpreted as the energy of the signal in the different scales relative to the Haar wavelet basis. Consider data containing information only at the finest scale: $X = \{1, \ -1, \ 1, \ -1, \ \cdots\}$. Then only the $d_1(n)$ coefficients are non-zero. Hence, S_j roughly corresponds to the energy at $2^{(j-1)}$ times the finest scale.

Note that the spatial support of the integrals of the process defining the wavelet coefficients at a certain scale is adapted to the particular scale. The short scales, that provide high frequency information, are defined in terms of consecutive integrals of narrow support. A plot of these difference coefficients reveals information about how the high frequency content of the data change with location.

4.3 The aerothermal data

4.3.1 Temperature and index of refraction fluctuations

Our objective is to estimate the spectrum of temperature data taken from the upper atmosphere. One motivation for our modeling and estimation is to be able to generate synthetic random media for the simulation of wave propagation in a turbulent atmosphere. Before we analyze the aerothermal data we explain briefly how velocity, temperature and index of refraction fluctuations are related to each other and how the Kolmogorov scaling theory enters in their description (Monin and Yaglom [21]; Strohbehn [31]).

The Kolomogorov theory is a phenomenological statistical description of the *velocity* field in the atmosphere. Based on a scaling argument, the mean-square velocity differences are described in a universal manner over a rather broad range of spatial scales, the inertial range. If we assume homogeneity, isotropy and incompressibility the result is that the structure function of the velocity has the form

$$E[(\mathbf{v_x}(\mathbf{x_0}+\mathbf{x})-\mathbf{v_x}(\mathbf{x_0}))^2] \;=\; C_{\mathbf{v}}^2|\mathbf{x}|^{2/3} \tag{4.4}$$

Here $\mathbf{v_x}$ is the velocity in the direction of the displacement $\mathbf{x}$. The parameter $C_{\mathbf{v}}^2$ is the velocity structure constant, a measure of the amount of energy in the inertial range, which is typically confined between an inner scale l_0 and an outer scale L_0.

The connection to temperature is through the theory of convection-diffusion of a passive scalar. It turns out (Monin-Yaglom [21]) that temperature fluctuations have also a structure function with Kolmogorov 2/3 scaling.

At optical frequencies the variations in the index of refraction δn are approximately

$$\delta n = -79P\frac{\delta T}{T^2}\times 10^{-6}$$

with P atmospheric pressure in millibars and T temperature in degrees Kelvin. Thus, in order to describe the spectrum of fluctuations in the refractive index we need only the spectrum of the fluctuations in the temperature. Wavelet scale spectra are used to analyze turbulence data in Hudgins, Friehe and Mayer [14].

The above model for refractive index fluctuations is used extensively to model atmospheric wave propagation. Variations in the turbulent character of the medium are typically modeled through variations in $C_{\mathbf{v}}^2$ only and not in the exponent, which is fixed at 2/3.

4.3.2 Data analysis of aerothermal data

We will analyze temperature data obtained by the Air Force high-altitude laser propagation and turbulence data collection effort. For a detailed discussion of recording procedures and analysis see Washburn et al. [34]; Papanicolaou et al. [34]; Rossi et al. [30]. A strong effort was made to provide high quality data that could be used to characterize the turbulent atmosphere. This unique data set cannot be maid generally available, but the above references provide together a fairly detailed account for the data. Here we take the data as our starting point and examine what analysis reveals about their structure. We are interested in particular in accounting properly for nonstationary effects. All calculations are carried out in MATLAB on a Silicon Graphics workstation.

In Figure 4.1 we show the temperature data, which has approximately 4.2×10^6 points. The spatial resolution is approximately 2cm. The data is, of course, quite noisy and it is part of our task to remove spurious noise effects in the estimation process.

In Figure 4.2 we show the first $21km$ of the temperature data along with $d_1, d_3, d_5, d_7, d_9, d_{11}, a_{11}$. The detail coefficients d_j carry information about the data on larger scales as j increases. For

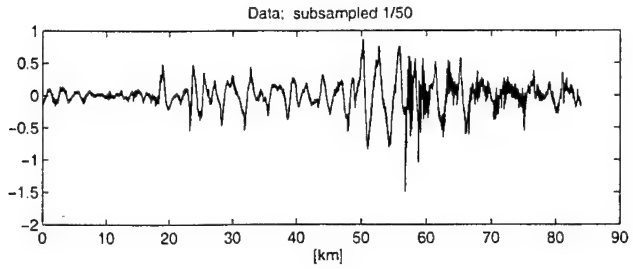

Figure 4.1: Top figure: the raw temperature data. The spatial resolution of the data is approximately 2cm.

example, d_7 shows successive differences of the temperature over distances of $2.56m$, after averaging over successive segments of length 1.28. Thus, as j increases the data are *lowpass* filtered with a filter of decreasing bandwidth and then *subsampled* before the differences are formed. It is clear that the visible periodic components seen in the d_1 coefficients cannot be attributed to turbulence or larger coherent structures in the atmosphere. In the estimation of atmospheric turbulence parameters these spurious features must be suppressed. In $d_5, \cdots$ the high frequency periodic noise component seen above has been effectively suppressed by the lowpass filtering.

Our main objective is now to examine whether the data can be modeled well by a 'power law' model over a subrange of scales. Recall that for such a process, the scale spectrum S_j is linear in a log-log plot, when the record is very long. In Figure 4.3 we show log-log plots of scale spectra over nonoverlapping segments of the data, with each segment having length $1.3km$. The top plot corresponds to the first half of the data whereas the bottom plot corresponds to the second half. Each plot contains scale spectral points over 16 scales, $1 \leq j \leq 16$. This corresponds to length scales from $l_1 = .04m$ to $l_{16} = 1.3km$. We take as abscissa the spatial frequency K_j

$$K_j \;=\; \frac{\pi}{\Delta x} 2^{1-j} \text{ [rad/m]} \;=\; 100\pi 2^{-j} \text{ [rad/m]}. \tag{4.5}$$

Note that the scale spectra show a distinct departure from power law behavior for scales below one meter ($K = 6$). For larger scales, power law behavior may be considered in the range between $2.5m$ to $80m$ ($.08 \leq K \leq 2.5$) approximately, which corresponds to the detail coefficients d_7 to d_{12}. The departure from power law behavior for the shortest scales is partly due to the influence of measurement noise. The first half of the data is less energetic than the second half and hence more noisy. The estimated intercept and slope for the log scale spectra depend on the particular segment of data used. We want to identify the part of this variability that is due to the nonstationarity of the process and minimize variability due to estimation errors.

For fractional Brownian motion the wavelet coefficients will be normally distributed. In Figure 4.4 we show a histogram of the wavelet coefficients at scale 8, normalized by a local estimate of the variance. The dashed line corresponds to a Gaussian distribution. In the bottom plot we show the autocorrelation of these wavelet coefficients, normalized by their variance. We plot the correlation in terms of the empirical variogram computed, as in (4.11) below. The dashed line is the theoretical correlation for fBm with Kolmogorov scaling, $H = 1/3$ (as defined in (4.13)). In Figure 4.5 we show an estimate of the structure function for $\log(d_j(n)^2)$; $7 \leq j \leq 9$. If the process had a pure power law spectrum over these scales we would see only a very small correlation. However, these quantities are correlated

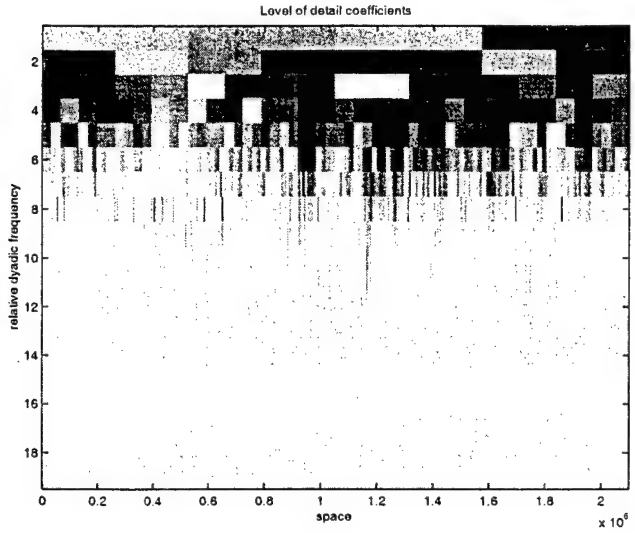

Figure 4.2: Haar wavelet coefficients for the first 21km of the data. The top left figure is the temperature data. The one below it is the d_1 detail coefficients. The third from the top is the d_3 and the bottom the d_5 detail coefficients. Note that the 4km burst seen in d_1 is not visible any more at the d_5 level, after four successive averagings of the data. The top figure on the right is the a_{11} coefficients and below it d_{11}, d_9, d_7.

on the order of km, indicating that we have a local power law structure.

Before we continue with the scale spectral analysis we note the following.

- Noise bursts in the data enter only in some of the detail coefficients, as can be seen from Figure 4.2. The criterion for selecting of the inertial range, implemented in the next section, will automatically restrict the scale range.
- The temperature data are not a stationary time series and they do not have stationary increments. Computing scale spectra over *long* segments, in which the process cannot be taken as stationary, gives a quantity that is hard to interpret. Even though the average slope of the log scale spectra over several segments is close to $-5/3$, as the theory of turbulence predicts, there is a lot of variability. A **local** power law model of the kind discussed in Section 4.4 is likely to fit the data better than the idealized power law model, with stationary increments.

We will estimate the scale spectrum of the data when we model it as a local power law, using the method described in Section 4 To start the estimation we must have rough estimates for the intervals of stationarity and for the exponent of the power law. In view of Figures 4.3, 4.4 and 4.5 we choose these estimates to be

- $(\hat{\varepsilon})^{-1} = 2km^{-1}$
- $H_0 = 1/3$ (Kolmogorov scaling) .

In the next section we develop a framework for estimation of local power law processes with varying inertial range and power law parameters. In Sections 4.5.1 and 4.5.2 we carry out the estimation. First we estimate the inertial range and then the power law parameters.

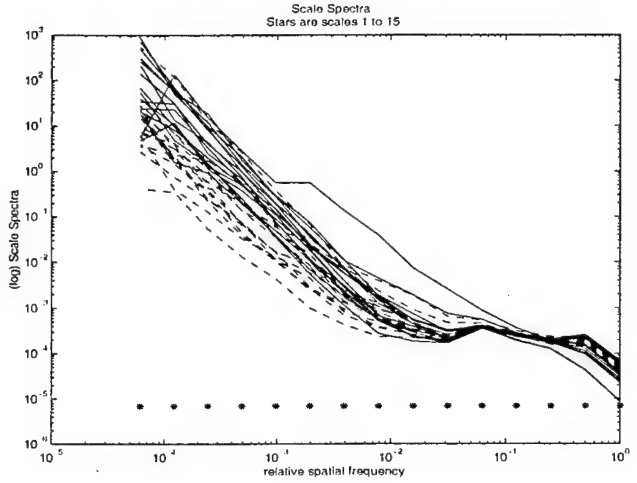

Figure 4.3: Scale spectra of $1.3km$ nonoverlapping segments of the data (2^{16} points per segment) obtained from the Haar wavelet decomposition. The top plot corresponds to the first half of the data whereas the bottom plot corresponds to the second half. The dashed line has slope $-5/3$ as in Kolmogorov spectra. The solid line is the average over the scale spectra of the different segments. After the averaging is done the scale spectra are plotted in log-log format.

4.4 Estimation of local power law processes

4.4.1 Modeling and segmentation

The fractional Brownian motion described in Section 2 is an idealization of a process with power law spectrum. It has stationary increments and if the power law is truncated at low frequencies then it is itself stationary. In most physical or financial applications where power law behavior is expected locally, the power law parameters will vary so the process cannot be stationary in the large. The aerothermal data provide an example. We would like to estimate the power law parameters over segments that are short enough so that they can be taken as constant but long enough so that their statistical estimates are stable. How are we to decide what is a good segmentation of the data in this vague sense? This is a very difficult problem that is rarely addressed in theoretical or applied studies of spectral estimation. In Mallat et al. [17] a class of locally stationary processes is introduced and an algorithm for finding intervals of approximate stationarity is developed. This method is based on an exhaustive search for an optimal segmentation, in a suitable sense, into intervals of stationarity. It does not work so well when the intervals of stationarity are all of roughly the same size, and when dealing with turbulence data. Thus, here we want to follow a somewhat different approach where we can take advantage of prior information about intervals of stationarity, as is the case of the aerothermal data.

To fix ideas we will consider estimation of parameters for a multifractional Brownian motion (mBm). This is a generalization of fractional Brownian motion where the parameters vary with location. In the time domain they have the representation, (Goncalves and Flandrin [9]; Peltier and Levy-Vehel [27])

$$B_\varepsilon(x) = \frac{\sigma_\varepsilon(x)}{\Gamma(H_\varepsilon(x)+1/2)} \int_{-\infty}^{0} [(x-s)^{H_\varepsilon(x)-1/2} - (-s)^{H_\varepsilon(x)-1/2}] dW(s) \qquad (4.6)$$

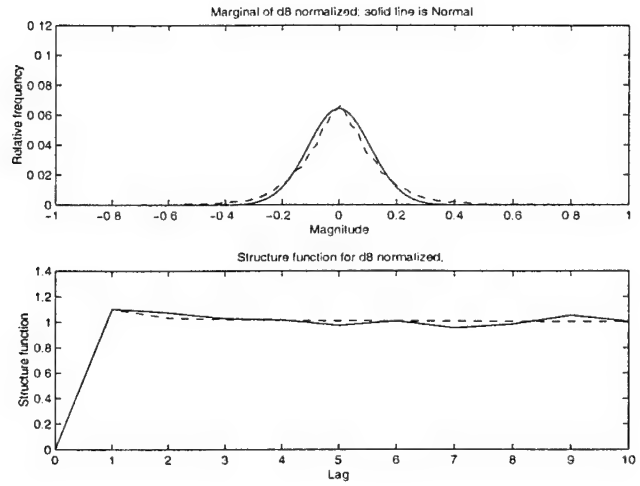

Figure 4.4: The top plot shows the empirical distribution of d_8. The solid line is a Gaussian distribution. The bottom plot shows the correlation of these wavelet coefficients. The dashed line is the theoretical correlation for fBm with $H = 1/3$.

$$+ \int_0^x (x-s)^{H_\varepsilon(x)-1/2} dW(s)$$

with W the standard Brownian motion and

$$H_\varepsilon(x) = H(\varepsilon x) \tag{4.7}$$
$$\sigma_\varepsilon(x) = \sigma(\varepsilon x) \tag{4.8}$$

where $H(\cdot)$ & $\sigma(\cdot)$ can be deterministic or random. For example, they can be stationary stochastic processes with smooth paths and decaying correlation functions, independent of the Brownian path $W(\cdot)$. When H and σ are constants then (4.6) is a time domain representation of the usual fractional Brownian motion.

The parameter ε^{-1} is a measure of the interval of stationarity in the sense that, as in Goncalves and Flandrin [9],

$$E[(B_\varepsilon(x) - B_\varepsilon(x-\Delta x))^2] \approx \sigma_\varepsilon^2(x)|\Delta x|^{2H_\varepsilon(x)}$$

for $\varepsilon\Delta x$ small. This means that for scales that are small compared to the interval of stationarity, the processes $B_\varepsilon(x)$ behaves locally like a fractional Brownian motion with parameters frozen at x.

In Section 4.4.3 we will describe a method that removes dependence of the estimated parameters on a prior estimate of the interval of stationarity. The basic idea is that we know roughly what $1/\varepsilon$ should be and how the estimation errors behave if the underlying process is fractional Brownian motion, given the segment size. We then filter out these estimation errors and get estimates that do not depend sensitively on the prior choice of the size of the interval of stationarity.

Another modification that is necessary in the nonstationary case is the identification of the inertial range over each interval of approximate stationarity. The error in the power law fit to the scale spectra, over a segment of data, depends on the scale range that is used. How do we select a range of scales for which the error in the fit is acceptable? In the next

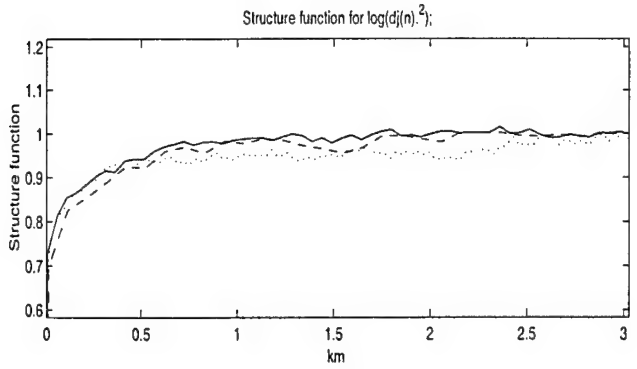

Figure 4.5: The figure shows an estimate of the structure function of $\log(d_j(n)^2)$ as function of $n\Delta x$ and with $7 \leq j \leq 9$. The magnitude of these quantities determine the scale spectrum and they decorrelate over a scale on the order of km. The dotted, dashed and solid lines corresponds respectively to scales 7,8 and 9.

section we introduce a criterion for selecting the range based on comparison with an ideal fractional Brownian motion.

4.4.2 Estimation of the inertial range

The power law behavior that we want to identify in the data is necessarily restricted to a finite set of scales, the inertial range, in each segment of stationarity.

Let 2^M denote the length of the data vector over the segment under consideration. For an ideal fractional Brownian motion with Hurst exponent H let S_i, $i = 1, \ldots, M$ be its wavelet scale spectrum. Then, for each subrange $\{i_1, \cdots, i_2\}$ the measure of misfit

$$r(i_1, i_2) \quad = \quad \sum_{i=i_1}^{i_2} [\log_2(S_i) - \log_2(\hat{S}_i]^2, \tag{4.9}$$

with $\hat{S}_i$ the power law estimated by weighted least squares, is a random variable whose law can be computed analytically in principle or numerically. It depends weakly on H so we fix it to equal some rough estimate $H = H_0$. For the aerothermal data of Section 4.3 we take $H_0 = 1/3$, the Kolmogorov exponent. Let $R(i_1, i_2)$ be the 90th percentile of the distribution of $r(i_1, i_2)$ with the value of the Hurst parameter equal to H_0. The scale range is now chosen as the *largest* range $\{i_1, \cdots, i_2\}$ for which $\tilde{r}(i_1, i_2) < R(i_1, i_2)$. Here $\tilde{r}(i_1, i_2)$ is the value of the error (4.9) obtained from the actual data.

In order to obtain stable power law parameter estimates in the regression we need a minimum number of scale range points. In the application to the aerothermal data introduced in Section 3 we choose to model in terms of a power law only over segments for which there are 5 or more points in the estimated scale range.

4.4.3 Segmentation independent power law estimation

Given a fixed segmentation of the data into approximate intervals of stationarity that is based on some prior information, we first calculate the inertial range as described in the previous section and then do the power law fit. The power law parameters are obtained by

weighted linear regression of the log scale spectrum, see Section 4.7.4. The estimated power law parameters depend on the segmentation. We will now describe a method with which this dependence can be removed.

The idea is to do a filtering of the parameter estimates in order to remove the variability that is segmentation dependent. From the theory of the power law estimators for fractional Brownian motion we know that the slope estimator has the form

$$\hat{p}^i = p^i + w^i \tag{4.10}$$

where p^i is the slope for the i'th segment and w^i the fluctuation due to the finiteness of the segment. We cannot take large segments, that reduce this error, because we are limited by the nonstationarity. The errors w^i are essentially uncorrelated over different segments and we have to construct a filter that will predict p^i from the estimates $\hat{p}^i$ by removing the noise w^i, to the extent possible. We assume that p^i is itself a stationary stochastic process, independent of the Brownian motion that generates the fractional Brownian motion. The p^i are the intrinsic variation of the power in the locally stationary fractional Brownian motion. The correlation length of the p^i must be longer than the segments used in estimating them in order to have approximate stationarity relative to the segmentation.

It can be shown using the results from Section 6 that w^i is close to being a white process. This is important because it allows us to estimate the autocovariance of p^i from the estimates $\hat{p}^i$, using the variogram, for example. Given estimates of the autocovariance of p^i and the variance of w^i we can design a minimum mean square error predictor or smoothing filter for $\hat{p}^i$.

The minimum variance unbiased filter for prediction of the parameter processes is as follows. We describe it in the context of the slope parameter, but the filtering of the log intercept is completely analogous. Let $\hat{\mathbf{P}} = (\hat{p}_i)$ be the vector of estimates, $\mathbf{P} = (p_i)$ the realization of the slope process and $\bar{\mathbf{P}} = (\bar{p})$ the constant mean. Then the filter Γ is a matrix that transforms $\hat{\mathbf{P}}$ into $\Gamma\hat{\mathbf{P}}$ in such a way that

$$E[||\Gamma\hat{\mathbf{P}} - \mathbf{P}||^2]$$

is minimized over all matrices Γ that also preserve the mean $\bar{\mathbf{P}}$ of $\mathbf{P}$, that is $\Gamma\bar{\mathbf{P}} = \bar{\mathbf{P}}$. Let C_p be the covariance matrix of $\mathbf{P}$. Then it easily follows that

$$\Gamma = (C_p + C_w)^{-1}[C_p + \mathbf{u}^T \otimes \bar{\mathbf{P}}]$$

where the vector $\mathbf{u} = (u_i)$ is given by

$$u_i = \frac{\bar{\mathbf{P}}_i - \bar{\mathbf{P}}^T(C_p + C_w)^{-1}C_{p,i}}{\bar{\mathbf{P}}^T(C_p + C_w)^{-1}\bar{\mathbf{P}}}$$

and C_w is the diagonal covariance matrix of the estimation errors w^i. Here $C_{p,i}$ is the $i-$th column of the matrix C_p and the superscript T stands for transpose. The slope and log intercept processes are filtered separately. Filtering of this kind is discussed in Ripley [32] and Cressie [3] for example.

Since the effect of the sample noise w^i in (4.10) is largely removed by the filtering procedure, the estimates of the parameter processes will be essentially independent of the prior choice of segmentation.

4.5 Application to aerothermal data

4.5.1 Estimation of inertial range

We estimate the set of scales where the process can be modeled as a 'power law'. Figure 4.3 shows that it varies with location. That is, the set of scales where the scale spectrum is

approximately linear is location dependent. There are two main reasons for this. First, the scale range where the physical process has power law spectrum varies and depends on the local intensity of the turbulence. Second, the set of scales that are affected by measurement noise varies depending also on the intensity of the turbulence.

We use the scheme described in Section 4.4.2 to estimate the inertial range. First, we choose a segmentation that is short relative to the prior estimate of the interval of stationarity. We choose segments of length 2^{15} points. Then we apply the algorithm of Section 4.4.2. For all scale ranges we measure the difference between the scale spectrum computed from the data and the fitted power law and choose the estimated scale range as the largest one for which this measure is within the 90th percentile of the corresponding measure for a realization of fractional Brownian motion.

The estimated 'effective inertial ranges' are shown in Figure 4.6 by the vertical solid lines. For each segment there is one vertical line showing the scales included in the corresponding effective inertial range. The segments consist of 2^{15} points and the maximum scale considered is therefore 14. Note that the more energetic second half of the data displays a more consistent power law behavior, as one would expect on physical grounds in fully developed turbulence.

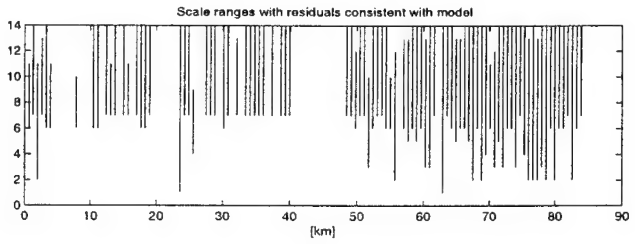

Figure 4.6: The vertical lines in the figure are the estimates of the location dependent inertial ranges. That is, the scales over which the observed process is approximately a power law. For each segment of length 2^{15} points there is one vertical line showing the scales included in the inertial range estimate.

The spectra computed with the estimated location dependent inertial ranges are shown in Figure 4.7, the top plot. They are plotted in a log-log format and shifted vertically to coincide at a center scale. We include only spectra that have at least 5 points. Note the fluctuations in the computed slopes. In Figure 4.7, bottom plot, we show the average of the spectra. The averaging is carried out *before* the log transformation. Note the excellent match with the Kolmogorov scaling law shown by the solid line. There is a slight deviation at the $5th$ scale. This corresponds approximately to the onset of the measurement noise caused by the airplane, see Figure 4.3.

4.5.2 Estimation of power law parameters

In the previous Section we estimated the inertial range for the scale spectrum, relative to a fixed segmentation. We will now estimate the power law parameters over this set of constrained scales. We use the method described in Section 4.4.3 for this purpose. Our main objective is to capture the intrinsic variation in the parameters. If we choose a coarse segmentation the variability of the estimates will be small. However, the estimated power law based on the scale spectrum may in this case be an average of power law parameters that vary within the section. This is illustrated in Figure 4.7. The average power law

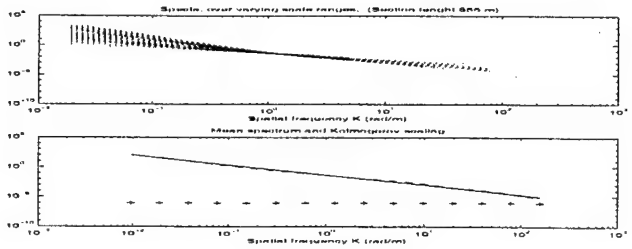

Figure 4.7: The top plot shows the computed scale spectra in each subsection, dotted lines. The estimates are based on the scale ranges shown in Figure 4.6. The bottom plot are the average of the (untransformed) spectra. Note the good match with the Kolmogorov scaling law shown by the solid line.

over the whole data set is very close to the Kolmogorov scaling law. However, within each section (see top plot) such a model must clearly be rejected. Therefore we must choose a segmentation that is not much larger than the interval of stationarity. The estimates should be independent of segmentation. That is, if we shorten the segments this should not lead to an increase in the variability of the estimated parameters.

To show that this is achieved by filtering we choose three segmentation lengths in addition to the one used in the previous section. We choose the following segmentations

$$160m\ (2^{13}\ \text{points}),\ 327m\ (2^{14}),\ 655m, (2^{15}),\ 1.31km\ (2^{16}).$$

There are 512, 256, 128, 64 nonoverlapping segments, respectively, in each case. For each segmentation we estimate inertial ranges for the scale spectrum as above. In Figure 4.6 we show the estimated ranges corresponding to segments of length $655m$.

We use the linear least squares regression

$$\log S_j^i \approx c^i + p^i \log_2(\frac{2^j}{50})$$

for each segment i, with j the scale in suitable units. In Section 4.7.4 we analyze the regression (4.11). The results of the estimation are shown in Figure 4.8. If the inertial range has fewer than 5 spectral points we do not estimate power law parameters and leave a gap in the figure.

We see from the figure that the estimated slopes, p, and the log intercepts, c, vary considerably over the 80 kilometer data set. They also depend on the segmentation, with the finer ones having larger fluctuations (dotted lines). Note also that the parameter estimates corresponding to the coarsest segmentation differ qualitatively from the others. This segment length is so long that intrinsic variation in the parameters are not captured appropriately. The difference between the parameter estimates for the finest segmentations is mainly due to a white noise estimation residual. For the log intercept process this residual is small and we have essentially obtained what we sought, a parameter estimate that is stable with respect to a shortening of the segmentation. However, for the slope estimate this residual is large. This leads us to the second step of the estimation. In this step we carry out a filtering procedure in order to remove the sampling variability that is segmentation dependent and particularly strong for the slope process p. We use the filtering described in Section 4.4.3. From the first step we obtained the estimates (in the case of the slopes)

$$\hat{p}^i \quad = \quad p^i + w^i \ .$$

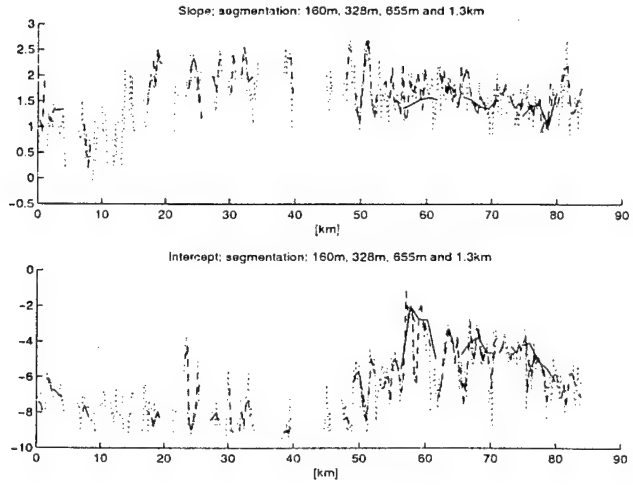

Figure 4.8: Top figure: slopes of log-log scale spectra from wavelet decompositions based on four different segment lengths. At the finest resolution the scale spectra are calculated over nonoverlapping segments 160m long. This is the dotted line that has the largest variations. At the next resolution the nonoverlapping segments are 327m long (plotted with a dashed line). The other two resolutions are 655m and 1.31km and are shown with dash-dotted and solid lines, respectively. The bottom figure is the same as the top but now for the log intercept of the scale spectra. The gaps correspond to inertial ranges with fewer than five spectral points.

The filter computes the minimum variance unbiased predictor of p^i given $\hat{p}^i$.

To construct the minimum variance unbiased filter we need the some additional estimates that we get from the process $\hat{p}^i$. We assume that the slope process is exponentially correlated. We need, therefore, its correlation length l_p and its variance σ_p^2

$$E[(p_i - \bar{p})(p_j - \bar{p})] \quad = \quad \sigma_p^2 \exp(-L|i-j|/l_p)$$

with L the length of the segments. Note that this model is intrinsic to the process and does not depend on the segmentation. As discussed above we shall model the sample noise process $\{w_i\}$ as white and we only need its level σ_w^2. We estimate the parameters σ_p^2, l_p and σ_w^2 using the empirical variogram.

For a time series $\mathbf{X} = (X_i)$ of size N the empirical variogram with lag j is defined by

$$V(j) = \frac{1}{2(N-j)} \sum_{k=1}^{N-j} (X_{k+j} - X_k)^2 \tag{4.11}$$

with dependence on the length of the data vector N not shown. Note that the variogram is essentially unaffected by a relatively slow variation in the mean $\bar{\mathbf{P}}$ of the process. The mean of the empirical variogram for the slope process $\hat{\mathbf{P}}$ is

$$E[V(j)] \quad = \quad \sigma_p^2(1 - \exp(-L|j|/l_p) + \sigma_w^2$$

and from this we obtain the parameter estimates by fitting to the empirical variogram. In particular, σ_w^2 is given by the vertical intercept since the process $\{w_i\}$ is white.

The estimated parameters are as follows:

- **For the slope**: Vertical intercept $\sigma_w^2 = 0.07$, horizontal asymptote level $\sigma_w^2 + \sigma_p^2 = 0.16$, and correlation length $800m$ (five segment lengths).
- **For the log intercept**: Vertical intercept $\tilde{\sigma}_w^2 = 0.1$, horizontal asymptote level $\tilde{\sigma}_w^2 + \tilde{\sigma}_c^2 = 3.0$, and correlation length $800m$ (five segment lengths) are the corresponding parameters.

These estimates are obtained using the finest segmentation, $160m$, and only the data in the last half section, the high turbulence section. The estimates were based on slope and log intercept processes obtained by regression as above, but for the *fixed* set of scales 7 to 12. In this case the magnitude of the estimation error does not depent on the segment. We show the correlation structure in Figure 4.9. The solid line is the fitted model. There are two parts to it, the sampling noise part (the intercept) and the exponential part corresponding to intrinsic variation in the parameters. The intercept part is seen to match well with that obtained from the asymptotic theory presented in Section 6 which predicts its value to be 0.07 for the slope and 0.05 for the intercept.

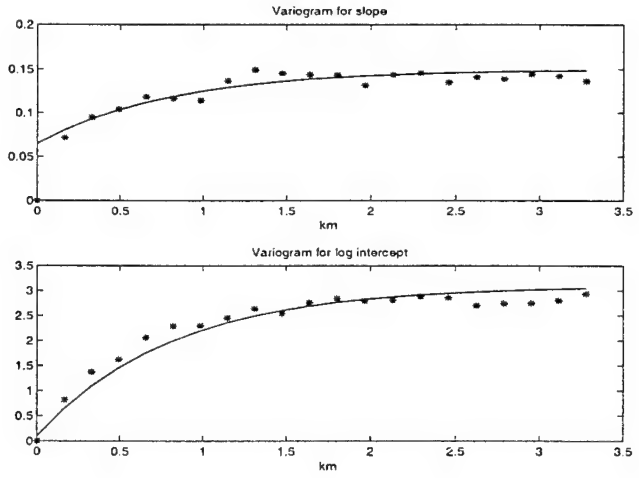

Figure 4.9: Variograms for the fluctuations of the slope (top) and log intercept (bottom) processes obtained from the temperature data. The stars are the variograms. The solid lines are fitted exponentials. We use slope and log intercept estimates from the data with the finest, $160m$, resolution.

Using the estimated model parameters we carry out the filtering to get a better estimate for the slope and log intercept processes. In Figure 4.10 we show these filtered slope and intercept processes. Note that after the filtering all three segmentations give essentially the same result; as expected. We do not include the coarsest segmentation since its segment length is long relative to the interval of stationarity and intrinsic variations in the parameters are being smoothed out.

We next simulate synthetic temperature profiles using the parameters estimated above. Recall that we only aim to model the process on the scales corresponding to the turbulent inertial range. We therefore *scale* filter both the aerotherman data of Figure 4.1 and the synthetic temperature profile so that only the coefficients in the Haar wavelet basis corresponding to the inertial range contribute. Figure 4.11 shows the scale filtered processes. The similarity between the processes is striking. Note the short section in the bottom plot

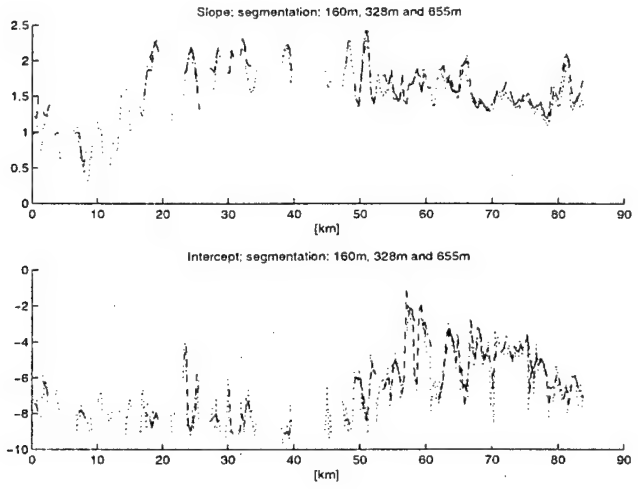

Figure 4.10: Filtered slope (top) and log intercept (bottom) processes of the actual data for the three finest segmentations. Note that the filtered processes for all three segmentations are essentially the same. The dotted line corresponds to the two finest resolutions. The dash-dotted and dashed curves correspond to the coarsest segmentations. The filtering has eliminated the differences in the slope and log intercept processes that are due to the segmentation (as in Figure 4.8) by removing the white noise component of the slope and log intercept fluctuations that is due to sampling. Note the closeness of the slope estimate to the Kolmogorov value 1.66 in the energetic, second half of the data. Note also the increased value of the log intercept, and its fluctuations, in the energetic second half. This is what is expected from physical considerations (Washburn et al. [34]).

with no data shown. This interval corresponds to a low intensity non-turbulent interval in the atmosphere where a laser beam propagates without much distortion due to medium heterogeneities. Next, we assess the accuracy of the parameter estimates by applying the estimation procedure to simulated data. We found that the standard deviation between the specified and estimated parameters for the local slope and log-intercept estimates to be .15 and .3 respectively.

4.6 Summary and conclusions

We have analyzed in detail estimation of fractional Brownian motion based on the scale spectrum. Moreover, we have generalized the estimation procedure to a local power law process. For such processes the power law itself (the exponent or slope) and the multiplicative constant (log intercept of the scale spectrum) are not constants but vary slowly. We estimate the slope and log intercept of the scale spectrum by appropriately segmenting the data and then removing segmentation effects by a filtering procedure. The slope and log intercepts themselves are modeled as stochastic processes. The estimation of the power law includes the identification of a location dependent inertial range, that is, the scale range where the process can be modeled as a power law.

We applied the estimation procedure to an important set of aerothermal data. We found that the *average* of the estimated slope process is close to the value predicted by the Kolmogorov scaling theory. To get a faithful representation of the heterogeneity in the data

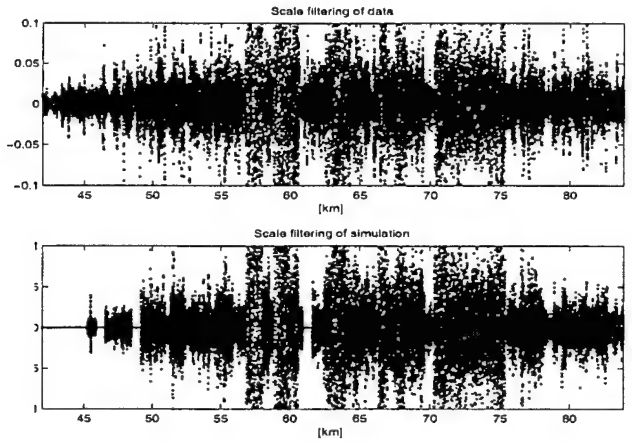

Figure 4.11: The *actual* temperature data set (top figure) obtained by synthesizing it from the detail coefficients in the range 6 to 11 of its Haar decomposition, corresponding to about 1 to 40 meters. Information from this range of scales enters into the estimates of the slope and log intercept processes. The bottom figure is the same as the top but for the *simulated* data. Note the striking similarity between the two figures.

it is however important to incorporate the local fluctuations around this value.

We generate synthetic temperatures in two different ways. First, the local power law process is simulated conditioned on the particular parameters estimated from the data (slope and log intercept). Then we get a faithful replication of the (scale filtered) temperature data. Second, the parameters are taken as random, that is, sampled from their model. Then the simulation is sample-wise very different from the actual data, but the statistics are faithfully reproduced. Such realizations can be used to define synthetic media for wave propagation codes. This is the application that motivated our investigation. A complete study of the effects of the heterogeneity in local power law model on wave propagation has yet to be carried out.

An important aspect of the model that we use is separation of scales in the variation of the estimated parameters (slope and log intercept) from the scale at which we sample the process.

4.7 On estimation of fractional Brownian motion

4.7.1 Statistics of wavelet coefficients for fBm

The scale spectrum is based on the wavelet coefficients. We now consider the statistics of the Haar wavelet coefficients for fBm. Next we will analyze the scale spectrum and power law parameter estimates based on these statistics. We assume that the data given to us is the wavelet approximation coefficients at level zero. That is, we assume that

$$a_0(n) \quad = \quad \int_{n-1}^{n} B_H(x)dx \ . \tag{4.12}$$

The wavelet coefficients are therefore normally distributed random variables with

$$\begin{aligned} E[d_j(n)] &= 0 \\ Var[d_j(n)] &= \sigma^2 \frac{(1-2^{-2H})}{(2H+2)(2H+1)} 2^{j(2H+1)} \\ Cor[d_{j_1}(n_1)d_{j_2}(n_2)] &= \frac{1}{8(2^{2H}-1)} |D/\sqrt{l}|^{2H+2} \{\delta^2_{l/D}\delta^2_{1/D}|x|^{2H+2}\}|_{x=1} . \end{aligned} \quad (4.13)$$

Here

$$l = 2^{j_2-j_1}, \quad j_1 \leq j_2 \quad (4.14)$$

is the relative scale,

$$D = |(2n_2-1)l - (2n_1-1)| \quad (4.15)$$

is the relative location and

$$\delta^2_d f(x) = f(x+d) - 2f(x) + f(x-d) \quad (4.16)$$

is the second order symmetric difference. These results are derived using (4.1) and self-similarity of fBm. Note that the expression for the correlation of the wavelet coefficients takes on a universal form depending only on the relative displacement in space and scale. The derivation of the precision of the power law estimators in Section 4.7.3 is based on (4.13), which was only known in special cases before (Tewfik and Kim [33]; Flandrin [7]).

Consider the correlation of wavelet-coefficients, when

$$\frac{D}{l} = |2^{j_2}(2n_2-1) - 2^{j_1}(2n_1-1)|2^{-j_2} \rightarrow +\infty$$

then

$$\frac{\delta^2_{l/D}}{(l/D)^2} \frac{\delta^2_{1/D}}{(1/D)^2}$$

is a forth order central difference operator and its expansion gives the asymptotic result

$$Cor[d^{n_1}_{j_1} d^{n_2}_{j_2}] = \frac{(H+1)(2H+1)H(2H-1)}{2(2^{2H}-1)} \left[\left(\frac{\sqrt{l}}{D}\right)^{2-2H} + O\left(\frac{\sqrt{l}}{D}\right)^{4-2H} \right] .$$

If the scales j_1 and j_2 are given, then for $n_2 \rightarrow \infty$ and n_1 fixed we have that $\frac{\sqrt{l}}{D} \approx \frac{1}{2n_2\sqrt{l}}$, whereas for $n_1 \rightarrow \infty$ and n_2 fixed we have $\frac{\sqrt{l}}{D} \approx \frac{\sqrt{l}}{2n_1}$. The correlation within a single scale is in particular

$$Cor[d^{n_1}_j d^{n_2}_j] = \frac{(H+1)(2H+1)H(2H-1)}{2(2^{2H}-1)} \left[\left(\frac{1}{2|n_2-n_1|}\right)^{2-2H} + O\left(\frac{1}{|n_2-n_1|}\right)^{4-2H} \right] \quad (4.17)$$

For general wavelets the following asymptotic result is presented in Tewfik and Kim (1992) and Flandrin (1992)

$$\begin{aligned} E[d^{n_1}_{j_1} d^{n_2}_{j_2}] &\sim O(|2^{j_2}n_2 - 2^{j_1}n_1|^{2(H-R)}) \\ &\text{for } |2^{j_2}n_2 - 2^{j_1}n_1| \rightarrow +\infty \end{aligned}$$

with R being the number of vanishing moments for the wavelet ($R = 1$ for Haar wavelets).

4.7.2 Statistics of the scale spectrum

Using the above results for the wavelet coefficients we get a characterization of the statistics of the scale spectral points. The mean is

$$\begin{aligned} E[S_j] &= E[d_j(n)^2] = \sigma^2 h(H) 2^{j(2H+1)} \\ &\propto \int_{-\infty}^{\infty} \sigma^2 |f|^{-(2H+1)} \frac{\sin^4(\pi 2^{j-1} f)}{(\pi 2^{j-1} f)^2} 2^j df \end{aligned} \tag{4.18}$$

where

$$h(H) = \frac{(1 - 2^{-2H})}{(2H+2)(2H+1)} . \tag{4.19}$$

The normalized variance is

$$\frac{Var[S_j]}{E[S_j]^2} = 2\frac{\sum_{n,m}(C^j_{nm})^2}{N_j^2 E[S_j]^2} = \frac{1}{N_j}\left\{ \frac{4}{N_j} \sum_{k=0}^{N_j-1} (N_j - k)\rho_H^2(k) - 2 \right\} \tag{4.20}$$

with $N_j = 2^{M-j}$, the number of detail coefficients at level j and 2^M the total length of the data. Note that here and in the sequel we suppress the dependence on M. The matrix $C^j = (C^j_{nm})$ in (4.20) is the covariance matrix of the wavelet coefficients at scale j, determined by (4.13), and $\rho_H(k)$ is the corresponding correlation coefficient, which depends only on $k = |n_1 - n_2|$ and H. Denote

$$g(H) = \lim_{N_j \to \infty} \left\{ \frac{4}{N_j} \sum_{k=0}^{N_j-1} (N_j - k)\rho_H^2(k) - 2 \right\} \tag{4.21}$$

then

$$\frac{Var[S_j]}{E[S_j]^2} \approx \frac{g(H)}{N_j} \tag{4.22}$$

for N_j large. The function $g(H)$ is computed numerically and is shown in Figure 4.12. It depends only weakly on the value of H, especially when $H \leq 1/2$ which is the case of interest to us. The asymptotic behavior (4.22) holds only when the correlation $\rho_H^2(k)$ decays to zero in an integrable way. This means that the Hurst exponent must be restricted to $H < 3/4$. In the Kolmogorov case $H = 1/3$, the correlation ρ_H decays like $k^{-4/3}$.

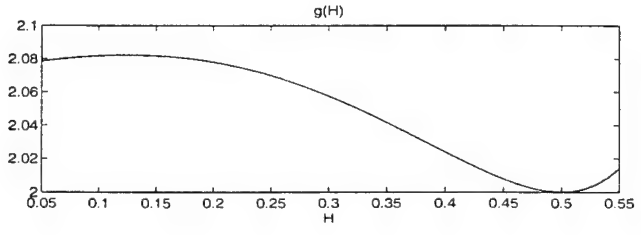

Figure 4.12: Plot of $g(H)$ showing how the relative variance of the scale spectrum depends on H.

Similarly, if $H < 3/4$, the normalized covariance can be expressed, for *fixed* scale separation, as

$$D_{j_1 j_2} \equiv \frac{Cov[S_{j_1} S_{j_2}]}{E[S_{j_1}]E[S_{j_2}]} = 2\frac{\sum_{n,m}(C_{nm}^{j_1,j_2})^2}{N_{j_1}N_{j_2}E[S_{j_1}]E[S_{j_2}]} \tag{4.23}$$

with C^{j_1,j_2} being the cross covariance between the wavelet coefficients at scale j_1 and j_2, determined by (4.13). The scale spectral points S_j are not uncorrelated for different j, as is sometimes assumed. For the power law parameter estimation we note that for fixed j_1 and j_2

$$D_{j_1 j_2} \equiv \frac{Cov[S_{j_1}, S_{j_2}]}{E[S_{j_1}]E[S_{j_2}]} \sim \frac{1}{\sqrt{N_{j_1}N_{j_2}}} \tag{4.24}$$

as N_{j_1} and N_{j_2} go to infinity. These results can be derived using (4.13).

4.7.3 Fluctuation theory for the scale spectra

In the least squares fit of the power law we will need the statistical properties of the logarithm of the scale spectra. We summarize the relevant facts in this section, with the details given in Appendix 1.

In the large N_j limit, the *distribution* of the scale spectral points is normal

$$\begin{aligned} S_j &= \bar{S}_j(1 + \frac{v_j}{\sqrt{N_j}}) \\ v_j &\sim \mathcal{N}(0, g(H)) \text{ as } N_j \to \infty \end{aligned}$$

with $\bar{S}_j \equiv E[S_j] = \sigma^2 h(H) 2^{j(2H+1)}$, and where h and g are defined by (4.21) and (4.19), respectively, and $\mathcal{N}(\mu, s^2)$ is the normal distribution with mean μ and variance s^2. The derivation of these results requires that $H \leq 1/2$. The covariance of the fluctuations is

$$Cov[\frac{v_j}{\sqrt{N_j}}, \frac{v_i}{\sqrt{N_i}}] = D_{ji} \tag{4.25}$$

with D_{ji} given by (4.24).

The fluctuations in S_j are small and in Appendix 1 we show that this leads to the asymptotic estimate

$$\log_2(S_j) \approx \log_2(\bar{S}_j) + \frac{v_j}{\sqrt{N_j}\ln(2)}. \tag{4.26}$$

In addition to showing that v_j is asymptotically normal, we also show in Appendix 1 that for any $j_1 < j_2$ fixed the random variables v_j, $j_1 \leq j \leq j_2$ are asymptotically jointly normal, as $N_j \to \infty$.

4.7.4 Estimators for the power law

Write (4.26) as

$$\begin{aligned} \log_2(S_j) &\approx \log_2(\sigma^2 h(H)) + j(2H+1) + \frac{v_j}{\sqrt{N_j}\ln(2)} \\ &= c + jp + \frac{v_j}{\sqrt{N_j}\ln(2)} \quad j_1 \leq j \leq j_2 \end{aligned} \tag{4.27}$$

with the slope p and log intercept c to be estimated from data, and $v_j/\sqrt{N_j}$ a fluctuation term that is characterized in the large N_j limit by the central limit theorem, as discussed in the previous section. In view of the above we can then use generalized least squares to estimate $\mathbf{b} = [c, p]^T$ as

$$\hat{\mathbf{b}} = (X^T D^{-1} X)^{-1} X^T D^{-1} \mathbf{Y} \tag{4.28}$$

with $\mathbf{Y} = [\log_2(S_{j_1}), \cdots, \log_2(S_{j_2})]^T$, and where $j_1, \cdots, j_2$ are the scales in the range under consideration,
the inertial range. The dependence on j_1, j_2 & M has been suppressed. For a discussion of generalized least squares see Hardle [12]. The design matrix X is defined as

$$X = \begin{bmatrix} 1 & j_1 \\ 1 & j_1 + 1 \\ \vdots & \vdots \\ 1 & j_2 \end{bmatrix} .$$

The matrix D is the normalized covariance matrix of the spectral points defined in (4.23). This matrix depends on the value of H. However this dependence is weak so we can use some rough estimate of H that is usually available, like $H = 1/3$ for the aerothermal data of Section 5. In view of (4.27) we find that the estimates of $\mathbf{b}$ have means

$$\begin{aligned} E[\hat{c}] &= \log_2(\sigma^2 h(H)) \\ E[\hat{p}] &= 2H + 1 \end{aligned} \tag{4.29}$$

and covariance

$$\begin{aligned} C_{\mathbf{b}} &= (X^T D^{-1} X \ln(2)^2)^{-1} \\ &= \frac{\ln(2)^{-2}}{[\sum\sum D_{ij}^{-1} \sum\sum D_{ij}^{-1}\, i\, j - (\sum\sum D_{ij}^{-1})^2]} \begin{bmatrix} \sum\sum D_{ij}^{-1} & -\sum\sum D_{ij}^{-1}\, i \\ -\sum\sum D_{ij}^{-1}\, i & \sum\sum D_{ij}^{-1}\, i\, j \end{bmatrix} \sim \frac{1}{N_{j_1}} \end{aligned} \tag{4.30}$$

for large N_{j_1}. From the above we arrive at the sought after parameter estimates

$$\hat{H} = (\hat{p} - 1)/2 \tag{4.31}$$

$$\widehat{\log_2(\sigma^2)} = \hat{c} - \log_2(h(\hat{H})) \; . \tag{4.32}$$

We next analyze the precision of these estimators. We find that the estimates $\hat{H}$ and $\widehat{\log_2(\sigma^2)}$ are normally distributed with variances

$$Var[\hat{H}] \approx C_{\mathbf{b}}(2,2)/4 \tag{4.33}$$

$$Var[\widehat{\log_2(\sigma^2)}] \approx C_{\mathbf{b}}(1,1) - 2C_{\mathbf{b}}(1,2)\ \log_2(h(H))' + C_{\mathbf{b}}(2,2)\ [\log_2(h(H))']^2 \tag{4.34}$$

for N_{j_1} large with $C_{\mathbf{b}}$ defined in (4.30) and h in (4.19). The variance of the estimators is of order $1/N_{j_1}$.

Long-memory processes can also be modeled via state space models. Maximum likelihood estimators (MLE) for such models are analyzed in Dahlhaus [4] and Fox and Taqqu [8].

4.7.5 Illustration of precision

The above result on the distribution of the estimators may be validated by numerical simulation. We generate synthetic realizations of fractional Brownian motion with known parameters. Then we use the above algorithm to estimate these parameters and compare

the precision of the estimates with the predicted precision. Actually, we do not simulate fractional Brownian motion but rather the observed sequence (4.12), the approximation coefficients at level zero. The synthetic realizations are generated by a simulation algorithm similar to the one discussed in Omre, Sølna and Tjelmeland [23].

In Figure 4.13 we compare the asymptotic law of the estimators with simulations. It is clear that the theoretical normal distribution predicts accurately the distribution of the estimators.

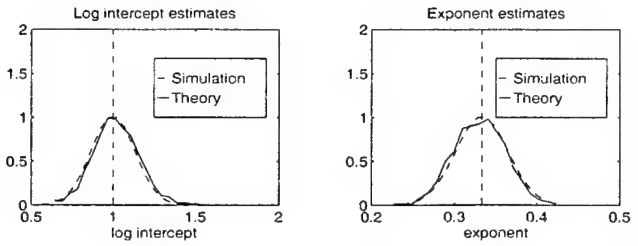

Figure 4.13: Distribution of power law parameter estimates. The parameters were estimated based on realizations of length 2^{10} with $H = 1/3$ and $\sigma^2 = 2$. The power law fitting is done over scales $1 \cdots 5$. The solid line is the empirical distribution associated with 1000 realizations, the dashed line is the theoretical distribution and the vertical lines are the specified parameters.

We show how the variance of the slope estimate $\hat{p}$ depends on the number of scales in the linear fit and the total number of data-points in Figure 4.14. The dotted and solid lines correspond to using respectively scales $1, 2, 3$ and scales $1, 2, 3, 4, 5$ and Hurst parameter $H = 1/3$. The crosses give the Cramer-Rao lower bound (Abry et al. 1995; Wornell and Oppenheim 1992): $1/(2^{M+2} \ln^2(2))$ for the case that the wavelet coefficients are uncorrelated. It is seen that only a few scales are needed for the variance of the slope estimator to be close to the bound.

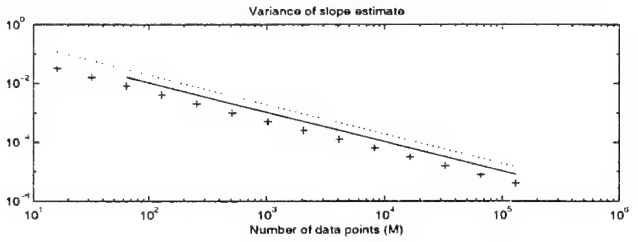

Figure 4.14: The variance of the slope estimate, computed by (4.33) with $H = 1/3$, is plotted as a function of the number of data points 2^M. The dotted line is for an estimate with three scales, the solid line with five scales. The crosses correspond to the Cramer-Rao lower bound. Note that even when the number of data points is not very large the estimate of the slope does not depend sensitively on the number of scales used.

Note that our objective is estimation of H when $H \approx 1/3$ and that our asymptotic result is valid only when $H < 1/2$. Several authors (Ninness 1998) have observed that slope estimators degrade when H become large ($H \approx 1$). This is because in that case the wavelet

coefficients exhibit long range correlations.

In the application of the estimation of the power law parameters to the aerothermal data in Section 5, which we model by a local fractional Brownian motion, we have to account for spurious noise effects. This noise affects the small scales mostly. We can make the power law parameter estimates more robust by letting the weight matrix D in (4.28) depend on an additive noise parameter which must be adjusted appropriately from rough prior data analysis. This is done in Section 4.5.2 without a detailed discussion.

4.8 Central limit theorem for scale spectra

In this appendix we derive a central limit theorem for the scale spectral points, S_j, and also the log transformed spectral points $\log_2(S_j)$, where

$$S_j = \frac{1}{N_j} \sum_{n=1}^{N_j} (d_j(n))^2$$

with $(d_j(n))_{n=1}^{N_j}$ the Haar wavelet coefficients of fractional Brownian motion at scale j with $H \leq 1/2$. The total number of data points is 2^M and $N_j = 2^{M-j}$. We will consider the limit $N_j \to \infty$. This means that M is large and that j is not too close to M, that is, the central limit theorem will not be valid for the large-scale spectral points S_j with $j \approx M$.

We will use the following version of the Berry-Esseen theorem (Feller [6]).

Let the y_i be independent random variables such that

$$E[y_i] = 0,\ E[y_i^2] = \sigma_i^2,\ E[|y_i^3|] = \rho_i$$

and define

$$s_n^2 = \sum_{i=1}^{n} \sigma_i^2,\ r_n = \sum_{i=1}^{n} \rho_i\ .$$

Let F_n be the distribution of the normalized sum $\sum_{i=1}^{n} y_i/s_n$.
Then for all x and n

$$|F_n(x) - N(x)| \ \leq\ 6\frac{r_n}{s_n^3} \tag{4.35}$$

where N stands for the mean zero, unit variance normal distribution.

4.8.1 Central limit theorem for S_j

To use this theorem we will first transform the sum of squares of wavelet coefficients to a sum of independent random variables. Denote the vector of wavelet coefficients at scale j by $d^j = [d_j(1), \cdots, d_j(N_j)]^T$ and the covariance matrix associated with d^j by C^j. Then d^j has the same law as

$$(C^j)^{1/2}[\eta_1, \cdots, \eta_{N_j}]^T$$

and in law

$$S_j \ = \ \frac{\bar{S}_j}{N_j} \sum_{i=1}^{N_j} \lambda_i^j \eta_i^2 \ = \ \bar{S}_j \left(1 + \frac{1}{\sqrt{N_j}} [\frac{1}{\sqrt{N_j}} \sum_{i=1}^{N_j} \lambda_i^j (\eta_i^2 - 1)] \right) \tag{4.36}$$

where η_i are independent zero mean and unit variance normal random variables, $\bar{S}_j = E[S_j]$ and λ_i^j are the eigenvalues of $C^j/\bar{S}_j$, that is the correlation matrix of d^j.

Let

$$Y_j \;=\; \frac{1}{\sqrt{N_j}} \sum_{i=1}^{N_j} y_i^j$$

with $y_i^j = \lambda_i^j(\eta_i^2 - 1)$. Note that the y_i^j are independent random variables such that

$$E[y_i^j] = 0,\; E[(y_i^j)^2] = 2(\lambda_i^j)^2,\;\; E[|(y_i^j)^3|] \leq 28(\lambda_i^j)^3 \;.$$

According to (4.35) we need only show that

$$J_j \;\equiv\; \frac{\sum_{i=1}^{N_j}(\lambda_i^j)^3}{[\sum_{i=1}^{N_j}(\lambda_i^j)^2]^{3/2}} \tag{4.37}$$

is small for N_j large.

Using (4.20) we find that

$$\sum_{i=1}^{N_j}(\lambda_i^j)^2 \;=\; \sum_{n,m}(C_{nm}^j/\bar{S}_j)^2 \;=\; N_j^2 Var[S_j]/(2\bar{S}_j^2) \;\approx\; N_j\; g(H)/2\;. \tag{4.38}$$

Below we show that

$$\lambda_i^j \;\leq\; K \tag{4.39}$$

for some constant $K \geq 1$ independent of N_j. Hence

$$\sum_{i=1}^{N_j}(\lambda_i^j)^3 \;\leq\; N_j K^3\;. \tag{4.40}$$

From (4.38) and (4.40) we find that

$$J_j \;\approx\; \frac{(2K^2/g(H))^{3/2}}{\sqrt{N_j}}$$

and goes to zero as $N_j \to \infty$. From the Berry-Esseen theorem we conclude that the distribution of

$$Y_j/\sqrt{g(H)} \;=\; \frac{\sum_{i=1}^{N_j}\lambda_i^j(\eta_i^2 - 1)]}{\sqrt{g(H)N_j}}$$

tends to the standard normal distribution as N_j becomes large.

Thus, for N_j large

$$S_j \;\approx\; \bar{S}_j(1 + \epsilon_j\sqrt{\frac{g(H)}{N_j}})$$

in law, with ϵ_j a standard normal random variable.

Let us now show that the estimate (4.39) is valid. The diagonal entries of the correlation matrix are all equal to one. By the Gersgorin disc theorem, $|\lambda_i^j - 1| \leq \sum_{n\neq i}|C_{in}|/C_{11}$. But the sum remains finite as $N_j \to \infty$ because we have assumed that $H \leq 1/2$ and so we can use (4.17). Rewriting this inequality with λ_i^j on the left side we get (4.39).

4.8.2 Central limit theorem for $\log_2(S_j)$

We consider next a central limit theorem for $\log_2[S_j]$. As in (4.36) we write the scale spectrum in terms of centered random variables Y_j

$$S_j = \bar{S}_j(1 + \frac{Y_j}{\sqrt{N_j}}) .$$

Taking logs and expanding in a Taylor expansion with remainder we get

$$\log_2(S_j) = \log_2(\bar{S}_j) + \frac{Y_j}{\sqrt{N_j}\ln 2} - \frac{Y_j^2}{2\xi(Y_j)^2 N_j \ln 2}$$

with

$$\xi(Y_j) \in \begin{cases} < 1, 1 + Y_j/\sqrt{N_j} > & \text{when } Y_j \geq 0, \\ < 1 + Y_j/\sqrt{N_j}, 1 > & \text{when } Y_j < 0. \end{cases}$$

We showed above that the central limit theorem holds for Y_j. We show below that $Y_j^2/(2\xi(Y_j)^2)$ is $O(1)$ as $N_j \to \infty$. We therefore, have a central limit theorem for $\log_2(S_j)$ as well.

By the Cauchy-Schwarz inequality

$$J_j \equiv E\left[|\frac{Y_j^2}{\xi(Y_j)^2}|\right] \leq \sqrt{E[\xi(Y_j)^{-4}]E[Y_j^4]} .$$

We show that $J_j = O(1)$ as $N_j \to \infty$. Consider first $E[Y_j^4]$. Using (4.39) we find

$$\begin{aligned} E[Y_j^4] &= E[(\frac{\sum_{i=1}^{N_j} \lambda_i^j(\eta_i^2 - 1)]}{\sqrt{N_j}})^4] \\ &\leq K^4(N_j E[(\eta_i^2 - 1)^4] + N_j(N_j - 1)6E^2[(\eta_i^2 - 1)^2])/N_j^2 = c_1 + c_2/N_j \end{aligned}$$

with c_i constants. Next consider

$$\begin{aligned} I_j &\equiv E[\xi(Y_j)^{-4}] \leq E[\xi(Y_j)^{-4} I_{(Y_j \leq 0)}] + 1 \\ &\leq E[(1 + Y_j/\sqrt{N_j})^{-4} I_{(Y_j \leq 0)}] + 1 \end{aligned}$$

with I_A the indicator function of the set A. In order to bound I_j we replace $1 + Y_j/\sqrt{N_j}$ by Z_j such that w.p.1 $Z_j \leq (1 + Y_j/\sqrt{N_j})$.

Note that

$$1 + Y_j/\sqrt{N_j} = \frac{\sum_{i=1}^{N_j} \lambda_i^j \eta_i^2}{N_j}$$

and that $\sum_{i=1}^{N_j} \lambda_i^j = N_j$, which is the trace of the correlation matrix for d^j. Let q be the number of eigenvalues that exceed $1/2$. In view of (4.39) we find

$$q \geq \tilde{N}_j = N_j(2K - 1)^{-1} \equiv N_j \tilde{K} .$$

Thus, we can define Z_j as

$$Z_j = \frac{1}{2}\frac{\sum_{i=1}^{\tilde{N}_j} \tilde{\eta}_i^2}{N_j} = \frac{\tilde{K}}{2}\frac{\sum_{i=1}^{\tilde{N}_j} \tilde{\eta}_i^2}{\tilde{N}_j}$$

Hence

$$I_j \leq E[Z_j^{-4} I_{(Y_j \leq 0)}] + 1 \leq (2/\tilde{K})^{-4} \tilde{N}_j^4 E[\tilde{Z}^{-4}] + 1$$

with

$$\tilde{Z}_j = \sum_{i=1}^{\tilde{N}_j} \eta_i^2$$

in law. The random variable $\tilde{Z}_j$ has law given by the Gamma density

$$\gamma_{(\alpha,\nu)}(x) = \frac{(\alpha)^\nu}{\Gamma(\nu)} x^{\nu-1} \exp(-\alpha x)$$

with parameters $\alpha = 1/2$ and $\nu = \tilde{N}_j/2$. It follows that for $\tilde{N}_j \geq 10$

$$E[\tilde{Z}^{-4}] = \frac{(\alpha)^\nu \Gamma(\nu-4)}{(\alpha)^{\nu-4}\Gamma(\nu)} = \frac{1}{(\tilde{N}_j-2)(\tilde{N}_j-4)(\tilde{N}_j-6)(\tilde{N}_j-8)} .$$

Hence, $I_j \leq K''$ and

$$J_j \leq \sqrt{K''(c_1/N_j + c_2)} \leq \tilde{K}$$

for $N_j \geq 10/\tilde{K}$.

From the above we conclude that for N_j large

$$\log_2(S_j) \approx \log_2(\bar{S}_j) + \epsilon_j \sqrt{\frac{g(H)}{N_j \ln(2)}}$$

in law, with ϵ_j a standard normal random variable.

4.8.3 Joint density of spectral points

We show that the spectral points are asymptotically, as $N_j \to \infty$, *jointly* normal. From this follows that the central limit theorem holds also for the power law parameter estimates. Consider the distribution of $Y = a_1 S_{j_1} + a_2 S_{j_2}$ with $a_1 \neq 0$ & $a_2 \neq 0$ and $j_1 < j_2$ fixed parameters. The central limit theorem for this quantity can be shown essentially as in Section 4.8.1. Let d^{j_1} and d^{j_2} be the vectors of wavelet coefficients at the two scales. Define

$$d = \begin{bmatrix} d^{j_1} \\ d^{j_2} \end{bmatrix}$$

and $\tilde{d} = Dd$ with D a diagonal matrix whose first N_{j_1} elements equal a_1 and last N_{j_2} elements equal $a_2 2^{j_2 - j_1}$. Then

$$Y = \tilde{d}^T \tilde{d} / N_{j_1} .$$

By a transformation to independent variables and an application of the Berry-Esseen theorem we find, as in (4.37), that we need to show

$$J \equiv \frac{\sum_{i=1}^{N_{j_1}+N_{j_2}} (\lambda_i)^3}{[\sum_{i=1}^{N_{j_1}+N_{j_2}} (\lambda_i)^2]^{3/2}} \tag{4.41}$$

is small for N_{j_1} large. Here λ_i are the eigenvalues of $Cov(\tilde{d}) = DCD$ with C the covariance matrix of d. Note first that from (4.20) it follows that

$$\sum_{i=1}^{N_{j_1}+N_{j_2}} \lambda_i^2 \;\geq\; (a_1)^2 \sum_{n,m} (C_{nm}^{j_1})^2 \;\approx\; (a_1)^2 N_{j_1} (\bar{S}_{j_1})^2 g(H)/2 \,.$$

Hence, (4.41) follows if we can bound λ_i uniformly with a bound independent of N_{j_1}. We find, using (4.13) and the Gersgorin disc theorem, that for some constant L and $1 \leq j \leq N_{j_1}$

$$|\lambda_j - a_1 \bar{S}_{j_1}| \;\leq\; L\bar{S}_{j_1}$$

since the rows of C are absolutely and uniformly summable with a bound that is independent of N_{j_1}. Hence $\lambda_i \leq \tilde{L}\bar{S}_{j_1}$ for some constant $\tilde{L}$. A similar argument holds for $N_{j_1} < j \leq N_{j_1} + N_{j_2}$. Therefore, (4.41) and the central limit theorem for Y follows.

Chapter 5

Spectral Analysis

5.1 Introduction

For a segmentation with segment length T and sample interval Δt, the measurable frequency range is $2\pi/T < \omega < \pi/\Delta t$, which corresponds to the scale range T to Δt. While Δ is usually dictated by the intrinsic bandwidth of the process being sampled or the instrumentation, the choice of T has always been somewhat arbitrary. The SpecLab procedure relies on matching scale spectra to a power-law model. In principle, standard spectral analysis could have been used, but there are compelling reasons to use scale spectra for this purpose. The material in this chapter has two objectives. The first is to demonstrate the problems that are encountered when standard spectral analysis procedures are applied to fBm. The second is to provide guidlines for translating the SpecLab structure function and Hurst exponent to spectral strength and power-law index.

To introduce the analysis consider a stationary power-law process that has an outer scale. In that case both the autocorrelation function and the spectral density function are well defined. Furthermore, the process itself admits a spectral decomposition. There is a wealth of material that describes standard analysis procedures that can be applied using discrete Fourier transforms (DFTs) to estimate the spectral density function (SDF). For reference, the essential elements of this material for our purposes are summarized in Section 5.2. The development in Section 5.2.2 shows that the structure function of a stationary power-law process admits the following limiting form for large outer scale:

$$\begin{aligned} D(y) &\approx \frac{C}{\sqrt{\pi}} \frac{\Gamma((3-\upsilon)/2)2^{2-\nu}}{(\upsilon-1)\Gamma(\nu/2)} |y|^{\nu-1} \\ &= \sigma^2 |y|^{\nu-1} \end{aligned} \tag{5.1}$$

The relation is valid for $1 < \upsilon < 3$ over the y range of scales that encompass the power-law segment. The unbounded power-law form of $D(y)$ does not have a Fourier transform, but (5.1) implies the following scale-free relation between the structure constant σ^2 and the spectral strength parameter C:

$$\sigma^2 = \frac{C}{\sqrt{\pi}} \frac{\Gamma((3-\upsilon)/2)2^{2-\nu}}{(\upsilon-1)\Gamma(\nu/2)}. \tag{5.2}$$

If the process is obtained from a probe sampling a two- or three-dimensional process via translation and path integration, additional scale-free transformations relate the one-dimensional parameters to an appropriate scale free characterizations of the actual medium.

In the remainder of this Chapter we first calculate the bias characteristics of the standard periodogram estimator when applied to fBm as opposed to a realizations of a stationary

process. The results show that the non-stationary characteristics of fBm introduce a more severe bias that is encountered with stationary processes. Furthermore, that bias will defeat attempts to estimate the spectral slope independent of the spectral strength. We then show that for the Haar wavelet applied to fBm the relation (5.2) is exact. The combination of these two observations strongly support the wavelet-based analysis.

5.1.1 Periodogram Bias for fBm

Consider the periodogram estimator $P_n = |\widehat{z}_n|^2 / N$, where $\widehat{z}_n$ is the discrete Fourier transform of a stationary process. The development in Section 5.2.2, suggests that $E[P_n] \approx C\omega^{-\nu}/\Delta t$. To test this conjecture, the expectation of the periodogrm can be computed from the defining properties of fBm. With some straightforward manipulations, it follows from the definition of the DFT and the fBm covariance function that

$$\begin{aligned} E\left[|\widehat{z}(n)|^2 / N\right] &= \sigma^2 \left(\textstyle\sum_{k=0}^{N-1} k^{2H}\right) \delta_n \\ &+\sigma^2 \textstyle\sum_{m=0}^{N-1} (1 - |m|/N)\, m^{2H} \cos(2\pi i n m/N). \end{aligned} \tag{5.3}$$

Figures 5.1 shows the result of averaging 10 periodogram estimates from independent 2^{12} point fBm realizations with $H = 1/3$. Superimposed on the averaged periodograms is the expectation derived from (5.3) with $\sigma^2 = 2^{-2dH}$, where d is the dyadic dimension and δ_n is the Dirac delta function. The nominal power-law with C derived from (5.2) has also been overlaid on the periodogram plot. We note first that the averaged periodogram agrees well with the expectation up to the highest frequencies. The departure comes from a small modification of the fBm process introduced to represent integration over the sample period rather than instantaneous sampling. More important, although the expectation appears to be reasonably power-law in form, the deviation from ideal power-law is frequency dependent and varies with the Hurst exponent. This behavior would not be expected for stationary processes as summarized in Section in 5.2.2.

5.1.2 Wavelets and Scale Spectra

Wavelet analysis has received considerable attention over the past decade, particularly with the discovery by Mallat [38] of the intimate relation between multiresolution filtering and wavelet decompositions. The book "Wavelets and Filter Banks" by Strang and Nguyen[39] covers the material in detail.

Continuous Wavelet Transforms

The continuous wavelet transform (CWT) of $x(t')$ is defined as

$$F_w(s,\tau) = \int_{-\infty}^{\infty} x(t') \frac{1}{\sqrt{s}} w\left(\frac{t'-\tau}{s}\right) dt', \tag{5.4}$$

where $w(t)$ is the "mother" wavelet. The parameter s is a scale parameter akin to period $(1/f)$ while τ locates the region where the scale information is extracted. To interpret (5.4), assume that $x(t)$ admits a spectral representation of the form

$$x(t) = \int \sqrt{Q(\omega)} \exp\{i\omega t\} d\zeta(\omega), \tag{5.5}$$

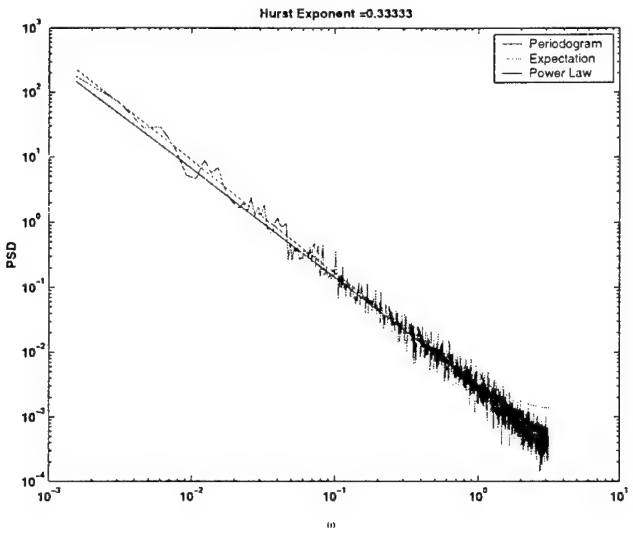

Figure 5.1: Average of periodograms from 10 independent realizations of fBm for $H = 1/3$. The magenta curve is the expectation value of each frequency. The blue curve is the ideal power-law.

where $d\zeta(\omega)$ has the formal "white-noise" property $E\left[d\zeta(\omega)d\zeta^*(\omega')\right] = \delta(\omega-\omega')/(2\pi)$. The well-known Fourier-transform relation

$$E\left[x(t)x^*(t')\right] = \int Q(\omega)\exp\{i\omega(t-t')\}\frac{d\omega}{2\pi} \tag{5.6}$$

follows from the white-noise property. Substituting (5.5) into (5.4) gives an equivalent spectral-domain representation of the CWT:

$$F_w(s,\tau) = \int_{-\infty}^{\infty}\sqrt{sQ(\omega)}\widehat{w}^*(s\omega)\exp\{i\omega\tau\}d\zeta(\omega). \tag{5.7}$$

Exploiting the white-noise property as before generates the τ-independent scale spectrum

$$E\left[\left|F_w(s,\tau)\right|^2\right] = \int_{-\infty}^{\infty}Q(\omega)s\left|\widehat{w}(s\omega)\right|^2\frac{d\omega}{2\pi}. \tag{5.8}$$

For a power-law process spectrum

$$E\left[\left|F_w(s,\tau)\right|^2\right] = \left(\int_{-\infty}^{\infty}\left|\omega\right|^{-\nu}\left|\widehat{w}(\omega)\right|^2\frac{d\omega}{2\pi}\right)Cs^{\upsilon}. \tag{5.9}$$

Since $s \propto 1/\omega$, the wavelet scale spectrum, unlike the fft-based estimator, evidently extracts the correct power-law form. Wavelets have the property that they integrate to zero, which implies that $\lim_{\omega\to 0}\widehat{w}(s\omega) = 0$. Thus, with an appropriate wavelet choice, the bias term may remain finite in spite of the singular behavior of the power-law $\omega = 0$. Ninness [40] and Abry et al.[1] have shown independently that the expectation of the scale spectrum for an fBm process does have the scale-free property implied by (5.9).

Discrete Wavelet Transforms

The discrete wavelet transform (DWT) is obtained by taking $t = k\Delta t$ and $s = 2^{j-1}\Delta t$, whereby

$$d_k^j \equiv F_w(2^{j-1}\Delta t, k\Delta t) = \frac{1}{\sqrt{2^{j-1}\Delta t}} \int_{-\infty}^{\infty} x(t')w((t'/\Delta t - k)/2^{j-1})\, dt'. \tag{5.10}$$

It is very inefficient to evaluate (5.4) by direct numerical integration, but following Mallat's [38] discovery of the intimate relation between multiresolution filtering and wavelet decompositions, the DWT can be computed efficiently without explicit use of the wavelet or the scale-function that generates it. Two sets of filter coefficients are applied recursively with downsampling to generate a wavelet scale decomposition that approximates (5.4) at logarithmically spaced scales. The results summarized here are developed in detail in the textbook by Strang and Nguyen [39].

Each wavelet has characteristics that strongly affect its applications. The MatLab Wavelet Tool Box provides a family of wavelets that are defined by orthogonal low- and high-pass filter coefficients Lo_D_m and Hi_D_m that can be generated by the function `orthfilt`. Both filters have L wavelet-dependent coefficients. The downsampled low-pass filter output at level (scale) j generates approximation coefficients a_k^j while the high-pass filter generates the corresponding detail coefficients d_k^j that form the DWT. The recursion is initiated at level 0 with the data samples:

$$a_k^0 = x_k \ for\ k = 0, 1, \cdots, N-1, \tag{5.11}$$

With $N = 2^M$ for $j = 1, \cdots, M$, the recursive filtering and downsampling operations are defined as

$$a_k^j = \sum_{m=0}^{L-1} Lo\_D_m a_{q(m)}^{j-1} \tag{5.12}$$

$$d_k^j = \sum_{m=0}^{L-1} Hi\_D_m a_{q(m)}^{j-1}, \tag{5.13}$$

where $q(m) = 2k - (m-1) + \alpha$ identifies the scale sample from the previous level that is multiplied by the mth filter coefficient. The $2k$ increment accounts for the downsampling. The offset α is a phase factor that determines where the current filter output is referenced. The recursion is not completely specified until the procedures for accommodating the first $L-1$ and the last $L-1$ samples are specified. The default MatLab procedure is to affix $L-1$ leading and trailing zeros to the data set. As a consequence, the approximation and detail coefficient vectors at level $j = 1$ are of length $L_D(1) = floor\left[(2^M + (L-1))/2\right]$, where *floor*[.] means the largest integer not exceeding the number in the brackets. The length of the detail coefficient vector for $j > 1$, as can be verified upon executing the MatLab Wavelet Tool Box `wavedec` routine, is

$$L_D(j) = floor\left[(2^M + (L-1)(2^j - 1))/2^j\right]. \tag{5.14}$$

Note that $L_D(j) \geq L_M(j) = 2^{M-j}$, where $L_M(j)$ is the nominal length of the data vector after downsampling. The orthogonality of the filters implies the norm preserving relation

$$\sum_{k=0}^{N-1} x_k^2 = \sum_{k=0}^{L_D(j)} \left(a_k^j\right)^2 + \sum_{m=1}^{j} \sum_{k=0}^{L_D(m)} (d_k^m)^2. \tag{5.15}$$

The wavelet scale spectrum is obtained by summing the intensity of a truncated set of the coefficients at each scale:

$$S_j = \frac{1}{L_M(j) - 1} \sum_{k=0}^{L_D(j)} U_k^j \left(d_k^j\right)^2, \tag{5.16}$$

with U_k^j symmetrically zero at the leading and trailing edge of the d_k^j vector to reduce its contributing length to $L_M(j)$.

5.1.3 The Haar Wavelet

Because the properties of fBm are defined in terms of its covariance function, we proceeds from relations such as (5.10) or (5.12) and (5.13). Closed-form solutions are difficult to come by, but the Haar wavelet has a particularly simple form:

$$w_{Haar}(t) = \begin{cases} 1 & for 0 \le t < 1/2 \\ -1 & for 1/2 \le t < 1 \end{cases}, \tag{5.17}$$

Substituting the Haar wavelet into (5.4), for example, yields

$$F_w(s,\tau) = \frac{1}{\sqrt{s}} \int_0^{s/2} [x(u+\tau) - x(u+\tau+s/2)]\, du. \tag{5.18}$$

Computation of the expectation of the scale spectrum is straightforward:

$$\begin{aligned} E\left[|F_w(s,\tau)|^2\right] &= \tfrac{\sigma^2}{2} \int_0^{1/2} \int_0^{1/2} \Big[|u-u'-1/2|^{2H} \\ &\quad + |u-u'+1/2|^{2H} - 2\,|u-u'|^{2H}\Big]\, du du' s^{2H+1} \end{aligned} \tag{5.19}$$

Carrying out the integrations and using the equivalence between (5.10) and (5.13) shows that

$$E\left[\left|d_k^j\right|^2\right] = \sigma^2 \frac{1 - 2^{-2H}}{(2H+2)(2H+1)} 2^{j(2H+1)} \tag{5.20}$$

One can also show that

$$|\widehat{w}(\omega)|^2 = \frac{\sin^4(\omega/4)}{(\omega/4)^2}. \tag{5.21}$$

Thus, from (5.9) the following equivalent expression involving the spectral strength parameter is obtained:

$$E\left[\left|d_k^j\right|^2\right] = \left(\int_{-\infty}^{\infty} |\omega|^{-(2H+1)} \frac{\sin^4(\omega/4)}{(\omega/4)^2} \frac{d\omega}{2\pi}\right) C 2^{j(2H+1)}. \tag{5.22}$$

Equating (5.20) and (5.22) gives an exact relation that defines σ^2/C:

$$C\left(\int_{-\infty}^{\infty} |\omega|^{-(2H+1)} \frac{\sin^4(\omega/4)}{(\omega/4)^2} \frac{d\omega}{2\pi}\right) = \sigma^2 \frac{1 - 2^{-2H}}{(2H+2)(2H+1)}. \tag{5.23}$$

Mathematica (courtesy of Raul Martinez at Vista) produced the following solution, which is evidently valid at $H = 0$:

$$\left(\int_{-\infty}^{\infty} |\omega|^{-(2H+1)} \frac{\sin^4(\omega/4)}{(\omega/4)^2} \frac{d\omega}{2\pi}\right) = \begin{cases} 1/12 & H = 1/2 \\ 2(2^{-2H} - 1)\cos(H\pi)\Gamma(-2(1+H)) & 0 <= H < 1/2 \\ & 1/2 < H < 1 \end{cases} \tag{5.24}$$

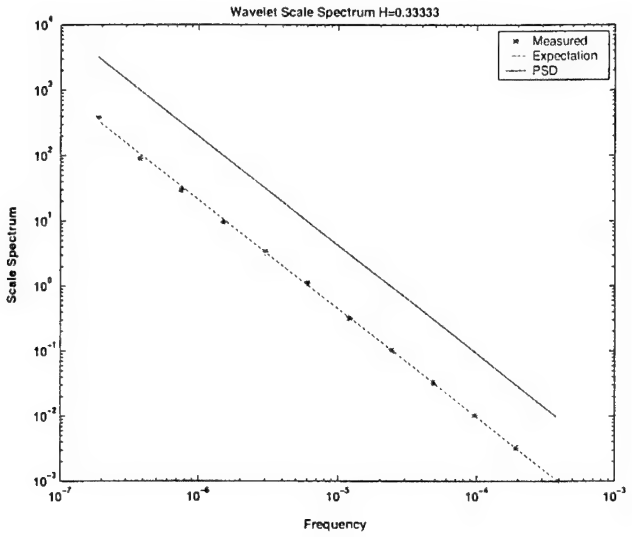

Figure 5.2: Average of wavelet scale spectra from 10 independent realizations of fBm for $H = 1/3$. The magenta curve is the expectation value for each scale converted to frequency. The blue curve is the ideal power-law.

Substituting from (5.2) for σ^2/C provides what we might expect to be an approximate relation:

$$\left(\int_{-\infty}^{\infty} |\omega|^{-(2H+1)} \frac{\sin^4(\omega/4)}{(\omega/4)^2} \frac{d\omega}{2\pi}\right) = \frac{\Gamma(1-H)2^{-2H}}{\sqrt{\pi}H\Gamma(H+1/2)} \frac{1-2^{-2H}}{(2H+2)(2H+1)}. \tag{5.25}$$

Figure 5.2 shows the raw scale spectra derived from fBm. The coefficients are plotted as red asterisks at the frequencies $\omega_{Nyquist}/2^{j-1}$. The solid red curve shows the theoretical expectation value derived from (5.20). The blue asterisks have the bias removed by using (5.23). The continuous blue curve is the theoretical SDF. In sharp contrast to the periodogram estimator, the scale spectrum captures the power-law. The offset from the ideal power law depends only on the Hurst exponent and is easily compensate. The scale spectrum removes the noise fluctuation without biasing the power-law index. Note that the norm preserving relation is of little use in calibrating the strength scale because it contains a non-stationary contribution from the average wavelet coefficients.

5.2 Background

The following material summarizes basic relations that are used in ScaleSpec.

5.2.1 Discrete Fourier Transforms

For a sequence of complex numbers $x(k)$ where $0 \le k \le N-1$ the discrete Fourier transform (DFT) and its inverse, as evaluated by the MatLab functions `fft` and `ifft` are defined as follows:

$$\widehat{x}(n) = \sum_{k=0}^{N-1} x(k) \exp\{-2\pi i n k/N\} \tag{5.26}$$

$$x(k) = \frac{1}{N} \sum_{n=0}^{N-1} \widehat{x}(n) \exp\{2\pi i n k/N\} \tag{5.27}$$

The Parseval relation

$$\sum_{k=0}^{N-1} |x(k)|^2 = \frac{1}{N} \sum_{n=0}^{N-1} |\widehat{x}(n)|^2 \tag{5.28}$$

is readily derived from (5.26) or (5.27).

If $x(t)$ and $\widehat{x}(\omega)$ are related via the continuous Fourier and inverse Fourier transformations

$$\widehat{x}(\omega) = \int_{-\infty}^{\infty} x(t) \exp\{-i\omega t\} dt \tag{5.29}$$

$$x(t) = \int_{-\infty}^{\infty} \widehat{x}(\omega) \exp\{i\omega t\} \frac{d\omega}{2\pi}, \tag{5.30}$$

it can be shown that $x_P(k\Delta t)/\Delta t$ and $\widehat{x}_P(n\Delta\omega)(2\pi/\Delta\omega)$ form an exact discrete Fourier transform pair. The periodic or "aliased" form of the continuous functions are defined as

$$x_P(x) = \sum_{m=-\infty}^{\infty} x(t + mT) \tag{5.31}$$

$$\widehat{x}_P(\omega) = \sum_{m=-\infty}^{\infty} \widehat{x}(\omega + 2\pi m/\Delta t) \tag{5.32}$$

where $\Delta t = T/N$ and $\Delta\omega = 2\pi/T$, whereby $\Delta t \Delta\omega = 2\pi/N$. The sampled functions themselves are the tapezoidal-sum approximations to the corresponding integrals. For a continuous Fourier transform pair, one chooses Δt and N so that the intervals $-T/2 \le t \le T/2$ and $-\pi/\Delta t \le \omega \le \pi/\Delta t$ contain the essential content of the corresponding function and its Fourier transform. The fact that natural reference for the functions is $t = 0$ or $\omega = 0$, whereas the discrete transforms place zero at the beginning of the interval establishes the need for a cyclic shift routine, which MatLab provides as `fftshift`.

5.2.2 Stationary Processes

A stationary stochastic process admits a spectral representation of the form

$$x(t) = \int_{-\infty}^{\infty} \sqrt{Q(\omega)} \exp\{i\omega t\}\, d\zeta(\omega), \tag{5.33}$$

where $d\zeta(\omega)$ has the formal "white-noise" property $E[d\zeta(\omega)\ d\zeta^*(\omega')] = \delta(\omega - \omega')/(2\pi)$. With $t = k\Delta t$, it follows from (5.26) that

$$\widehat{x}(n\Delta\omega) = \int_{-\infty}^{\infty} \sqrt{Q(\omega)} \frac{1 - \exp\{iT(\omega - n\Delta\omega)\}}{1 - \exp\{i\Delta t(\omega - n\Delta\omega)\}} d\zeta(\omega). \tag{5.34}$$

The raw periodogram estimator is defined as

$$P_n = |\widehat{x}_n|^2 / N. \tag{5.35}$$

The expectation of the periodogram is readily computed by using the white-noise property:

$$\begin{aligned} E\left[|\widehat{x}_n|^2/N\right] &= \tfrac{1}{N}\int_{-\infty}^{\infty} Q(\omega)\frac{\sin^2\left(\frac{T}{2}(\omega-n\Delta\omega)\right)}{\sin^2\left(\frac{\Delta t}{2}(\omega-n\Delta\omega)\right)}\frac{d\omega}{2\pi} \\ &\approx Q(n\Delta\omega)/\Delta t. \end{aligned} \tag{5.36}$$

The approximation holds for large N. Note that DFTs satisfy the Parseval relation

$$\frac{1}{N}\sum_{n=0}^{N-1}|\widehat{x}_n|^2 = \sum_{k=0}^{N-1}|x_k|^2. \tag{5.37}$$

Upon taking expectations and using, (5.36) we find that

$$\sum_{n=0}^{N-1} Q(n\Delta\omega)/\Delta t = N\left\langle x^2\right\rangle \tag{5.38}$$

or

$$\sum_{n=0}^{N-1} Q(n\Delta\omega)\frac{\Delta\omega}{2\pi} = \left\langle x^2\right\rangle. \tag{5.39}$$

That is, in expectation for large N the sum of the periodogram estimator is the discrete approximation to the corresponding integral relation for the SDF of a stationary process.

Power SDFs and Structure Functions

The follow SDF form is often used because it admits both a power-law regime and an analytic inverse[41]

$$Q(\omega) = C\left[\frac{2^{1-\upsilon/2}\left(q_s q_L\right)^{-\nu/2}}{\Gamma(\nu/2)}\right]\sqrt{1+(\omega/q_L)^2}^{-\nu/2}K_{\nu/2}\left(\frac{q_L}{q_s}\sqrt{1+(\omega/q_L)^2}\right). \tag{5.40}$$

We will now use this form to develop a relation between the structure constant and the spectral strength parameter. For small arguments $K_\nu(x) \approx (1/2)\,\Gamma(\nu)\,|x/2|^{-|\nu|}$. Thus, as long as $q_L << \omega << q_s$ and $q_L/q_s << 1$ (5.40) has the desired power-law form

$$Q(\omega) \approx C\omega^{-\nu}. \tag{5.41}$$

This "self-similar" Fourier transform is

$$R(y) = \frac{C}{\sqrt{\pi}}\frac{1}{2^{(\upsilon-1)/2}\Gamma(\nu/2)}\sqrt{r^2+(q_L y)^2}^{(\nu-1)/2}K_{(\nu-1)/2}(\sqrt{r^2+(q_L y)^2})/q_L^{\upsilon-1}, \tag{5.42}$$

where $R(y) = E\left[x(t)x^*(t')\right]$ and

$$r = q_L/q_s.$$

Unlike the SDF, the covariance function does admit a scale free power-law form. Consider that,

$$E[|x|^2] = R(0) \approx \frac{C}{\sqrt{\pi}}\frac{\Gamma((\nu-1)/2)}{\Gamma(\nu/2)q_L^{\upsilon-1}},$$

which is dominated by the outer-scale wavenumber through the factor $q_L^{1-\upsilon}$.

The coherence properties of power-law process with $\upsilon > 1$ are better characterized by the structure function

$$D(y) = E[|x(t) - x(t')|^2] = 2(R(0) - R(y)) \tag{5.43}$$

$$= \frac{2C}{\sqrt{\pi}} \frac{N}{2^{(\upsilon-1)/2}\Gamma(\nu/2)}$$

$$\times \left[1 - \sqrt{r^2 + (q_L y)^2}^{(\nu-1)/2} K_{(\nu-1)/2}(\sqrt{r^2 + (q_L y)^2})/N\right] / q_L^{\nu-1}, \tag{5.44}$$

where

$$N = r^{(\nu+1)} K_{(\nu-1)/2}(r) \approx \Gamma((\nu-1)/2) 2^{(\nu-1)/2}. \tag{5.45}$$

The term in square brackets converges to zero as q_L approaches zero. Thus, an application of LHopital's rule yields the asymptotic approximation

$$D(y) \approx \frac{C}{\sqrt{\pi}} \frac{\Gamma((3-\upsilon)/2) 2^{3-\nu}}{(\upsilon-1)\Gamma(\nu/2)} |y|^{\nu-1}$$

$$= \sigma^2 |y|^{\nu-1} \tag{5.46}$$

Bibliography

[1] Abry, P., Goncalves, P., and Flandrin, P., (1995), "Wavelets, Spectrum Analysis and $1/f$ Processes," in *Wavelets and Statistics,* eds. A. Antoniadis and G. Oppenheim, Springer Lecture Notes in Statistics 103, Springer Verlag, pp. 15-29.

[2] Asch, M., Kohler, W., Papanicolaou, G., Postel, M., and White, B., (1991), "Frequency Content of Randomly Scattered Signals," in *Siam Review,* 33, pp. 519-626.

[3] Cressie, N., (1993), *Statistics for Spatial Data,* Wiley New York.

[4] Dahlhaus, R., (1989), "Efficient Parameter Estimation for Self-similar Processes," in *Annals of Statistics,* 17, pp. 1749-1766.

[5] Feder, J., (1988), *Fractals,* Plenum Press, New York.

[6] Feller, W., (1970), *An Introduction to Probability Theory and its Applications,* Vol II, Wiley.

[7] Flandrin, P., (1992), "Wavelet Analysis and Synthesis of Fractional Brownian Motion," in *IEEE Transactions on Information Theory,* 38, pp. 910-917.

[8] Fox, R., and Taqqu, M., (1986), "Large-sample Properties of Parameter Estimates for Strongly Dependent Stationary Gaussian Time Series," in *Annals of Statistics*, 14, pp. 517-532.

[9] Goncalves, P., and Flandrin, P., (1992), "Scaling Exponents Estimation from Time-scale Energy Distributions," in *IEEE International Conference on Acoustics, Speech and Signal Processing,* ICASSP-92, San Francisco, pp. V.157-V.160.

[10] Goncalves, P., and Abry, P., (1996), "Multiple Window Wavelet Transform and Local Scaling Exponent Estimation," in Research Report, INRIA.

[11] Hall, P., Koul, H.L., and Turlach, B.A., (1997), "Note on Convergence Rates of Semi-parametric Estimators of Dependence Index," in *Annals of Statistics,* 25, pp. 1725-1739.

[12] Hardle, E., (1991), *Smoothing Techniques,* Springer Verlag.

[13] http://www-stat.stanford.edu/ wavelab

[14] Hudgins, L., Friehe, C.A., and Mayer, M.E., (1993), "Wavelet Transforms and Atmospheric Turbulence," in *Physical Review Letters,* 71, pp. 3279-3282.

[15] Kaiser, G., (1994), *A Friendly Guide to Wavelets,* Birkhäser.

[16] Kent, J.T., and Wood, A.T.A., (1997), "Estimating the Fractal Dimension of a Locally Self-similar Gaussian Process by Using Increments," in *Journal of the Royal Statistical Society B,* 3, pp. 679-700.

[17] S. Mallat, G. Papanicolaou and Z. Zhang, Adaptive Covariance Estimation of Locally Stationary Processes, Annales of Statistics, 26, pp. 1-47, 1998.

[18] Mallat, S., and Zhang, Z., (1993), "Matching Pursuit in a Time Frequency Dictionary," in *IEEE Transactions on Information Theory,* 38, pp. 3397-3415.

[19] V. Kruger, C. Rino, G. Papanicolaou and K. Sølna, "Analysis of Aerothermal Data," Vista Research Inc. Report, 100 View St., Mountain View CA 94041, 1998.

[20] Mandelbrot, B.B., and Van Ness, J., (1968), "Fractional Brownian Motion, Fractional Noises and Applications," in *SIAM Review,* 10, pp. 422-437.

[21] Monin, A.S. and Yaglom, A.M., (1971), *Statistical Fluid Mechanics: Mechanics of Turbulence.* Vol. 1. The MIT Press.

[22] Ninness, B., (1998), "Estimation of 1/f Noise," in *IEEE Transactions on Information Theory,* 44, pp. 32-46.

[23] Omre, H., Sølna, K., and Tjelmeland, H., (1993), "Simulations of Random Functions on Large Lattices," in *Geostatistics,* Eds. A. Soares, pp. 179-199, Kluwer Academic Publishers.

[24] G. Papanicolaou and K. Sølna, (1999) Wavelet Based Estimation of Local Kolmogorov Turbulence, submitted for publication JASA.

[25] Papanicolaou, G., Sølna, K., and Washburn, D., (1998), "Segmentation Independent Estimates of Turbulence Parameters," in *SPIE AeroSense Meeting,* Orlando Florida.

[26] G. Papanicolaou, K. Sølna and C. Rino, (1998) Vista Research Technical Report no. 2096 TM-98-001, 17.

[27] Peltier, R.F., and Levy-Vehel, J., (1995), "Multifractional Brownian Motion: Definition and Preliminary Results," Research Report, INRIA, 1995.

[28] Percival, D.B., and Guttorp, P., (1994), "Long-memory Processes, the Allan Variance and Wavelets, in *Wavelets in geophysics,* Eds. E. Foufoula-Georgiou and P. Kumar, pp. 325-344, Academic Press.

[29] Ripley, B., *Spatial Statistics,* Wiley, New York, 1981.

[30] Rossi, L., Kaiser, G., Washburn, D., (1998), "Recovery of Kolmogorov Statistics in Thermal Mixing in the Troposphere: The Hazards of Real Data," SPIE Meeting Orlando Florida.

[31] Strohbehn, J.W., (1978), *Laser Beam Propagation in the Atmosphere,* Springer Verlag, 1978.

[32] Robinson, P.M., (1995), "Log-periodogram Regression of Time Series with Long Range Dependence," in *Annals of Statistics,* 23, pp. 1048-1072.

[33] Tewfik, A.H., and Kim, M., (1992), "Correlation Structure of the Discrete Wavelet Coefficients of Fractional Brownian Motions," in *IEEE Transaction on Information Theory,* 38, pp. 904-909.

[34] Washburn, D., Banton, D.W., Brennan, T.T., Brown, W.P., Butts, R.R., Coy, S.C., Dueck, R.H., Koenig, K.W., Masson, B.S., Peterson, P.H., Praus, R.W., Tyler,G.A., Venet, B.P., and Weaver, L.D., (1996), "Airborne Laser Extended Atmospheric Characterization Experiment (ABLE ACE).", Technical report, Phillips Laboratory, Kirtland Air Force Base NM 87117-5776.

[35] Wang, Y, Cavanaugh, J.E. and Song, C., (1997), "Self-similarity Index Estimation via Wavelets for Locally Self-similar Processes," preprint, Department of Statistics, University of Missouri, Columbia, MO.

[36] Wornell, G.W., (1996), *Signal Processing with Fractals, a Wavelet Based Approach,* Prentice Hall.

[37] Wornell, G.W., and Oppenheim, A.V., (1992), "Estimation of Fractal Signals from Noisy Measurements Using Wavelets," in *IEEE Transactions on Signal Processing,* 40, pp. 611-623.

[38] S. Mallat, (1989) "A Theory of Multiresolution Signal Decomposition: The Wavelet Representation," in *IEEE Transactions on Signal Processing,* 11, pp. 674-693.

[39] Gilbert Strang and Truong Nguyen, (1992) *Wavelets and Filter Banks,* Wellesley-Cambridge Press, Wellesey MA.

[40] Brett Ninness, (1998) "Estimation of $1/f$ Noise," in *IEEE Trans. Inform. Theory,* 44, pp. 32-45.

[41] I. P. Shkarofsky, (1968) "Generalized Turbulence Space-Correlation and Wave-Number Spectrum-Function Pairs," in *Canadian J. Phys.* 46, pp. 2133-2153.

A-1Filt_Par

```
   Prediction of a process (s).
   Model:
          y = s + n = sm + sr + n
          n  - white noise (not stationary)
          s=sm+sr  with sm (constant) mean value
Usage:
   function    sp=Filt_Par(ind,y,vs,vn,l)

   Input: y    -  the observations                          column vector
          ind  -  argument vector (in sampling units)            "
          vs   -  variance of sr (sr being zero mean)       scalar
          vn   -  variance of 'measurement noise' n         column vector
          l    -  correlation range of sr in sampling units scalar
          (sr  stationary, n white not stationary)

   Output: sp  -  filtered version of y (prediction of s)
```

A-2GetParproc

```
Estimates and returns the power law parameter processes
given the segmentation, the scale spectra in the (spatial) segments
and the estimates of the inertial range.

Usage
    P=ScaleSpec(Z)
Input
    Z      - Matlab data structure containing spectra
             and inertial ranges. Initialized by InitSpec,
             ScaleSpec and InertialSpec (see also InitZ).

Output
    P      - The estimated parameter process

See Also: ScaleSpec ScfiltSpec SynthSpec
```

A-3GetVario

```
The variogram of the input process is estimated interactively.

Usage
    [intcept l v]=GetVario(y,titles)
```

```
Input
    y      -  the input data vector
    titles -  title string

Output
    l       -  estimate of the correlation range
    v       -  estimate of the variance
    intcept -  estimate of the intercept

See Also:  VarioSpec  VarioEst
```

A-3Get_Inertial

```
Estimates the inertial ranges given the scale spectra
in the set of segments and the length of the data vector
from which the scale spectra have been computed.
The estimation is done by comparing deviation of the log scale
spectrum from a linear log spectrum with the mean value
of this measure for Brownian motion.
Usage
     [inertial]=Get_Inertial(scspect,dyad);
Inputs
        scspect  - the set of scale spectra (#seg by #scales vector)
        dyad     - dyadic dimension of original data vector
Outputs
        inertial - the inertial ranges (#seg by 2 vector)

See Also:   InertialSpec

Parameters:
Refres          %  This matrix is stored on file: Refres
                   and contains the measure of deviation
                   for Brownian motion.
                   Dimensions is maxdyad by maxdyad with first index
                   corresponding to dyadic dimension and  second index to
                   size of inertial range.
 mins           %  Minimum number of scales in inertial range (> 1)
```

A-3HelpSpec

```
Gives online help for the main menu SpecLab options

Usage
     HelpSpec

See Also:  Main
```

```
The fields of Z are:
data          - the data vector
wavec & wavel - c & l from wavedec (length of data is l(length(l) )
nseg          - number of (uniform) segments
                in segmentation (scalar)
scspect       - scale spectrum
                (nseg by m array; [short to long scales];
                note that m is number of scales stored in
                wavec, which is 'length(wavel)-2').
inertial      - inner and outer scales in the segments
                (nseg by 2 array; [inner outer])
parproc       - the exponent and intercept estimates in segments
                (nseg by 2 array; [H interc])
filtpar       - parameters used in filtering of parproc
                (1 by 6 array;
                [intceptH varH corrlengthH ...
                intceptLogInt varLogInt corrlengthLogInt])
filtparproc   - filtered parameter process
trueparproc   - true parameter process (if process is simulated)

See Also:  SpecLab  Main
```

A-3Linreg

```
Estimates the power law parameters for the scale spectrum.
Usage
      [mspect,c,H]=Linreg(spect,low,high)

Input
               spect      - scale spectrum (column vector)
               low high   - inertial range used in estimation
Output
               mspect     - estimated model spectrum
               c          - estimated log intercept
               H          - estimated Hurst exponent

See Also:  ProcSpec
```

A-3Main

```
Main is part of SpecLab's  GUI driven interface that allows the user
to apply the components of SpecLab.
Main presents the user with the main menu that allow him or her
to apply the different estimation or plotting capabilities
of SpecLab. These are implemented by intermediate level
routines that call SpecLab's basic or tool routines.
```

```
Usage
     Z=Main(Z)

Output
          Z  - Matlab data structure conaining the analyzed
               process and its spectral information
               (see InitZ for format).

See Also: SpecLab Z   HelpSpec InertialSpec ProcSpec ScaleSpec
                      ScfiltSpec SmoothSpec SynthSpec VarioSpec
```

A-3MakeRefres

```
Computes the percentail of the residual of the scale spectrum relative to
the estimated linear model for various dyadic lengths of data
and sizes of the scale range. Result is used when inertial range is
estimated.

Usage
       MakeRefres

Outputs
   The matrix Refres is stored on the file Refres
   with storage format (ascii). Refres is a maxdyad by maxdyad
   array reshaped to linear form for storage.

See Also:   Get_Inertial

Parameter
```

A-3ProcSpec

```
Estimates plots and returns the power law parameter processes
given the segmentation, the scale spectra in the (spatial) segments
and the estimates of the inertial range.

Usage
    Z=ScaleSpec(Z)
Input
    Z      - Matlab data structure containing spectra
             and inertial ranges. Initialized by InitSpec,
             ScaleSpec and InertialSpec (see also InitZ).

Output
    Z      - The input Matlab data structure with
             the parameter processes added.

See Also:  Main
```

A-3ReadSpec

```
Reads data vector
Usage
     [Z,path]=ReadSpec(mode)
Inputs
    mode       - Type of data input
                 1: binary
                 2: ascii

Output
    Z          - Speclab data structure
    path       - path is 0 if no file was read

See Also:   SpecLab initZ getdat
```

A-3ScaleSpec

```
Computes plots and returns the wavelet scale spectrum
given the data and its wavelet decomposition. The
user can choose the number of segments in a uniform
segmentation of the data.

Usage
    Z=ScaleSpec(Z)
Input
    Z       - Matlab data structure containing data vector and
              its wavelet decomposition. Initialized
              by InitSpec (see also InitZ).

Output
    Z       - Matlab data structure that contains scale filtered
              data, its wavelet transform, the chosen segmentation
              and scale spectra in segments.

See Also   Main
```

A-3Scale_Filt

```
Low pass scale filtering of data
Usage
    [X,c,l]=scale_filt(c,l,inner);
Inputs
```

```
    c,l          -  wavelet transform obtained from wavedec
    inner        -  the inner scale used in filtering

Outputs
    c,l          -  low pass truncated wavelet transform
    X            -  low pass filtered data

See Also: ScfiltSpec
```

A-3ScfiltSpec

```
Scale filters data, plots them
and returns data-structure with spectral information.

Usage
    Z=InitSpec(Z)
Inputs
    Z       - Data structure containing spectral information
              (see InitZ for format).

Output
    Z       - Matlab data structure that contains a scale filtered
              version of input data.


See Also:  Main
```

A-3SegSim

```
  Simulates a locally stationary power law
Usage
    [z]=SegSim(dyad,pv,iv)
Inputs
       dyad   - dyadic dimension of simulation grid
       pv - Hurst process
       iv - log intercept process

Outputs
       z  - the simulated process (2^dyad by 1 vector)

See Also:  SynthSpec
```

A-3SimExp

```
  Simulates the locally stationary power law parameters.
  The model is a truncated Gaussian exponentially correlated
  stochastic process.
Usage
     [pv,iv]=SimExp(dyad,dyadl,Hm,Hs,Is,mode)
Inputs
       dyad   - dyadic dimension of parameter process
       dyadl  - dyadic dimension of corrlation length
       Hm     - mean of Hurst parameter
       Hs     - relative fluctuations in Hurst parameter
       Is     - relative fluctuations in log intercept
       mode   - optinal parameter
                mode : 1 - Triangular
                       2 - Gaussian correlation
                       3 - Exponential correlation

Outputs
       pv - Hurst process
       iv - log intercept process

See Also:  SynthSpec
```

A-3SmoothSpec

```
The power law parameter estimates are smoothed according
to the model estimated for their stochastic variations.
The smoothed are plotted optionally with the unsmoothed
versions.

Usage
    Z=SmoothSpec(Z)
Input
    Z      - Matlab data structure containing
             the (unfiltered) parameter processes and
             variogram parameters for their spatial variation,
             (see also InitZ).

Output
    Z      - The input Matlab data structure with
             the smoothed parameter processes added.

See Also:   Main
```

A-3SpecLab

```
SpecLab is an GUI driven interface that allows the user
to apply the components of SpecLab to a set of test
```

```
data sets or to simulated data sets whose parameters are
determined by the user. The user can alternatively load
his own dataset.
Using the GUI interface the user can estimate a Local Power
Law model for the data and also plot the dataset or
its spectrum in various ways.

Usage
     Z=SpecLab

Output
           Z  - Matlab data structure conaining the analyzed
                process and its spectral information
                (see InitZ for format).

See Also   InitZ Main
```

A-3Spect

```
Computes the wavelet scale spectrum
given the wavelet decomposition and the number of
segments in a uniform segmentation of the data.

Usage
    [scspect]=Spect(c,l,nseg)
Input
    c & l          - c & l from wavedec
    nseg           - number of (uniform) segments
                     in segmentation (scalar)

Output
    scspect        - scale spectrum
                     (nseg by m array; [short to long scales];
                     note that m is number of scales stored in
                     c, which is 'length(l)-2').

See Also:  ScaleSpec ScfiltSpec SynthSpec
```

A-3SynthSpec

```
Simulates a locally stationary power law.
The user specify the power law parameters from a simple model.
The intercept and Hurst exponent of the power law are taken to
be realizations of a stochastic process.
Also inner and outer scales are specified.
First a pure power law is simulated. Information
in scales beyond the inertial range is then tapered.
```

```
Usage
    [Z]=SynthSpec
Output
    Z      - Matlab data structure containing the simulated data
             vector and its spectral information
             (see InitZ for information about the fields).

See Also:    main
```

A-3Taper

```
  Tapers the locally stationary power law according to
  inner and outer scales with Gaussian tapering.
Usage
    [z]=Taper(z,ins,outs)
Inputs
       z    - the process
       ins  - the inner scale
       outs - the outer scale

Outputs
       z    - the tapered process

See Also:  SynthSpec
```

A-3VarioEst

```
Computes the variogram of the input process
and fit it to a vertically shifted  exponential model using least squares.
Usage
     [intcept l v vario]=VarioEst(y,maxlag);
Inputs
   y      - process for which the variogram is computed
   maxlag - the maximum lag for which the variogram is computed
Outputs
   intcept - estimated intercept
   l       - estimated correlation length
   v       -     "     variance
             The fitted variogram model is:   intcept+v*(1-exp(-x/l))
   vario   - the empirical variogram of y

See Also:   GetVario regmodel
```

A-3VarioSpec

```
Estimates the variogram or structure function of the
the power law parameter processes. The estimate
can interactively be modified by the user.
Usage
     [Z]=VarioSpec(Z);
Input
    Z       - Matlab data structure containing
              the (unfiltered) parameter processes,
              (see also InitZ).

Output
    Z       - The input Matlab data structure with
              the variogram parameters added.

See Also  Main
```

A-3WriteSpec

```
Reads data vector
Usage
         WriteSpec(Z)
Inputs
    Z  -  Matlab data structure with process
          (see InitZ for format)

See Also:  main InitZ writedat
```

A-3aero

```
This workout  illustrates how the figures in the paper:

   Wavelet based estimation of local Kolmogorov turbulence
               by  George Papanicolaou and
                         Knut Solna

can be generated using SpecLab. It also serves as an introduction
to SpecLab itself.

Usage
    Z=aero

Output:    Z - data structure with aerothermal data
              (see InitZ for format)

See Also:  SpecLab InitZ
```

A-3displayP

```
Plots the power law parameter processes
Usage
     displayP(Z,mode)
Inputs
    Z        -  Data structure containing data and spectral information
    mode     -  type of plot
                 1 : Plot unsmoothed parameters
                 2 : Plot smoothed and unsmoothed parameters
                 3 : Plot smoothed parameters

See Also:  Main InitZ ProcSpec SmoothSpec
```

A-3displayS

```
Plots the set of scale spectra
Usage
     displayS(scspect,N,mode,inertial)
Inputs
    scspect       -  scale spectrum
                     (nseg by m array; [short to long scales];
                     with m the number of scales and nseg the
                     number of spatial segments.
    N             -  length of data vector on which the scale
                     spectrum is based.
    mode          -  type of plot:
                      1 - color image
                      2 - graphs
                      3 - color image with inertial range
                      4 - graphs with inertial range
    inertial      - inner and outer scales in the segments
                    (nseg by 2 array; [inner outer])

See Also:  Main InertialSpec ScaleSpec SynthSpec
```

A-3displaySyn

```
Plots simulated process and parameters
Usage
    displaySyn(X,pv,iv)
Inputs
    X         - simulated process
    pv        - the Hurst process
```

```
    iv        - the log intercept process

See Also: Main SynthSpec
```

A-3displayVario

```
Plots variogram
Usage
    displayVario(model,vario,titles)
Inputs
    model      - model variogram
    vario      - empirical variogram
    intcept    - the itercept of the variogram
    titles     - the title string

See Also: Main GetVario
```

A-3displayW

```
Plots level of detail coefficients
Usage
    displayW(c,l)
Inputs
    c,l         - Wavelet decomposition


See Also: Main  ScfiltSpec
```

A-3displayX

```
Plots data vector
Usage
    displayX(X,titlestr)
Inputs
    X      - The data
    titlestr  -  title of plot

See Also:  Main  ScfiltSpec
```

A-3getdat

```
Reads data vector
```

```
Usage
     [Z,path]=getdat(filen,path,mind)
Inputs
    filen   -  file name
    path    -  path
    mind    -  minimum dyadic length of data-vector
    mode    -
               1:  binary
               2:  ascii
Output
    Z         - Data vector
    path      - path is 0 if no vector was read

See Also   ReadSpec  InitZ
```

A-3hfunc

```
Computes the function h(H) that is involved in the definition of
the mean and variance of scale spectral points.

Usage
    h=hfunc(H)
 Input:        H     - the Hurst exponent
 Output        h(H)  - scaling factor for mean and variance
                       of scalespectral points.

See Also: Linreg
```

A-3regmodel

```
Gives model variogram or structure function

Usage
     y=regmodel(beta,x);
Inputs
   beta      - correlation length
   x         - lag
Outputs
   y         - value of variogram

See Also:   VarioEst
```

A-3showinput

```
Shows the input menu with a paricular entry marked

Usage
        showinput(opt)

Input:
        opt - the menu entry that is to be illustrated next

See Also:   aero
```

A-3showmenu

```
Shows the main menu with a paricular entry marked


Usage
        showmenu(opt)

Input:
        opt - the menu entry that is to be illustrated next

See Also:   aero
```

A-3sim_ob

```
  Simulates OBSERVED fBm
  The process is scaled so that the value of the
  structure function at maximum lag (lag=2^d) is 1
  and condition on the process being zero at
  the 'zero'th value of the index.
  The measurement model corresponds to the observations
  being integrals of the fBm over unit intervals.

  Input :  d    - dyadic dimension
           H    - Hurst exponent!
  Output:  xold - Simulated sequence (2^d by 1 vector)

  Parameters:  D - dyadic dimension of supergrid in simulation
               l - parameter that determines the SIZE
                   of the conditioning set in the simulation.
                   (simulation ACCURACY and also TIME
                   increases with the value of these
                   two parameters). Note paremeters
                   need to satisfy 2^D > 2*l > 2.
```

A-3simcoef

```
Computes coefficients used by sim_ob in the simulation
of observed fBm.

Input :  n1,n2   - dimensions of conditioning sets
         del     - lag between conditioning nodes
         H       - the Hurst coefficient
Output:  c1,c2   - c1,c2 coefficients of conditioning nodes
         s       - conditional standard deviation of simulation
                   node.

See Also: sim_ob
```

A-3vfunc

```
Computes the value of the structure
function for fBm assuming a measurement
model where integrals of B over unit intervals
are observed. (value computed assuming \sigma^2=1)

Useage:    function       v=vfunc(lag,H)


Input:        H        - the Hurst exponent
              lag      - separation distance at which structure
                         function is computed (NB an integer)
Output        v        - value of structure function

See Also:   simcoef sim_ob
```

A-3writedat

```
Writes data vector
Usage
     [path]=writedat(filen,path,Z)
Inputs
    filen   -  file name
    path    -  path
    Z       - Matlab data structure with process
              (see InitZ for format)

Output
    path    - path=0 if file not propely written

See Also:  WriteSpec  InitZ
```